

GALAXY POPULATIONS AND EVOLUTION IN CLUSTERS III. THE ORIGIN OF LOW-MASS GALAXIES IN CLUSTERS: CONSTRAINTS FROM STELLAR POPULATIONS

CHRISTOPHER J. CONSELICE¹, JOHN S. GALLAGHER, III², ROSEMARY F.G. WYSE³*Accepted to the Astronomical Journal**Draft version October 28, 2018*

ABSTRACT

Low-mass galaxies in nearby clusters are the most numerous galaxy type in the universe, yet their origin and properties remain largely unknown. To study basic questions concerning these galaxies we present the results of a survey designed to constrain the characteristics and properties of the stellar populations in a magnitude complete sample of low-mass cluster galaxies (LMCGs) in the center of the Perseus cluster. Using deep, high-quality WIYN UBR images to obtain photometric and structural properties, we demonstrate that the 53 LMCGs in our sample have a significant scatter about the color-magnitude relationship at $M_B > -15$. By comparing single-burst stellar population models to our photometry, we argue that stellar populations in LMCGs all have ages > 1 Gyrs, with redder LMCGs containing stellar metallicities $[Fe/H] > -0.5$. By assuming that the colors of LMCGs reflect metallicity, and have co-evolved with the giant ellipticals, we find a wide range of values, from solar to $[Fe/H] \sim -3$. We argue from this that LMCGs have multiple origins, and fundamentally differ from Local Group dwarf spheroidals/ellipticals. The inferred lower metallicities of the bluer LMCGs implies that these are possibly primordial galaxies formed through self-enrichment and stellar feedback provided by winds from supernova. We also investigate several other formation scenarios for these LMCGs, including: self-enrichment induced by the confinement of metals in halos by the intracluster medium, in situ formation out of intracluster gas, systems with extreme dark halos, and as remnants of previously higher mass systems. We conclude that roughly half of all low-mass cluster galaxies in the center of Perseus have stellar populations and kinematic properties, as discussed in previous papers in this series, consistent with being the remnants of stripped galaxies accreted into clusters several Gyrs ago.

1. INTRODUCTION

Faint low-mass galaxies, especially those found in groups and clusters, are the most common galaxy type in the local universe, yet their nature remains elusive (e.g., Ferguson & Binggeli 1994). Because they are so common, these low-mass cluster galaxies (LMCGs) likely hold answers to some of the ultimate questions of how galaxies form and evolve. They are also the least massive galaxies known, whose nature is important for understanding hierarchical galaxy formation (e.g., White & Frenk 1991).

In Cold Dark Matter (CDM) cosmological models, containing a bottom up formation scenario for structure (e.g. White & Rees 1978), low-mass galaxies should be the oldest objects in the universe from which all other galaxies formed. While observations now reveal that stars in low-mass galaxies are potentially younger, on average, than giant elliptical galaxies (Rakos et al. 2001) there are a plethora of theories, both cosmological and evolutionary, for explaining how low-mass galaxies formed, generally within the CDM milieu (e.g., Dekel & Silk 1986; Silk, Wyse & Shields 1987; Babul & Rees 1992; Kepner, Babul & Spergel 1997; Mao & Mo 1998; Moore et al. 1998; Natarajan, Sigurdsson & Silk 1998; Ferrera & Tolstoy 2000; Cen 2001)

The traditional approach to studying low-mass galaxies

is to examine them in the Local Group (LG). It is now well established that LG dwarf elliptical and dwarf spheroidal galaxies have varying star formation histories, with metal-poor populations as old as classical halo globulars, but also with evidence for star formation occurring as recently as 2-3 Gyrs ago (see Mateo 1998 and van den Bergh 2000 for reviews). There are also some low-mass LG galaxies, such as Sagittarius, that contain surprisingly metal-rich populations given their luminosities (e.g., Ibata, Gilmore & Irwin 1995). Because LG dEs are close we can resolve their stellar populations, and thus we know much more about them than we do LMCGs, including their internal kinematics and star formation histories. Many of the lowest mass galaxies in the LG, such as Draco and Ursa Minor, have very high inferred central M_{total}/L ratios (Kleyna et al. 2002), and apparently contain the densest dark matter halos of all known galaxies, in qualitative agreement with the original CDM predictions (e.g., Lake 1990). Low-mass galaxies in clusters however have different kinematic and spatial properties than these LG systems (e.g., Conselice et al. 2001a) suggesting they might have a different formation scenario.

We can learn more about the formation of low-mass galaxies and their role in cosmology and large mass galaxy evolution by studying them where they are most abundantly found, in galaxy clusters. The high abundance of

¹California Institute of Technology, Mail Code 105-24, Pasadena, CA²Department of Astronomy, University of Wisconsin, Madison 475 N. Charter St. Madison, WI, 53706-1582³Department of Physics & Astronomy, The Johns Hopkins University

low-mass, or dwarf, galaxies in clusters was first pointed out by Reeves (1956), who studied them in the Virgo cluster, and by Hodge (1959, 1960) in the Fornax cluster. Soon after it was realized that both dwarf irregular-like (gas rich systems with star formation) and dE-like (gas poor systems with little star formation) objects exist in clusters (Hodge, Pyper & Webb 1965). Later, it became clear that these dwarfs are not clustered around giant galaxies as they are in groups (Reeves 1977), revealing perhaps a fundamental difference in origin. The modern study of LMCGs began with detailed optical and infrared observations of individual Virgo dwarfs (e.g., Bothun & Caldwell 1984; Bothun et al. 1985; Ichikawa, Wakamatsu & Okamura 1986; Gallagher & Hunter 1986; Bothun & Mould 1988), and extensive catalogs of dwarfs in nearby clusters (e.g., Bingelli, Sandage & Tammann, 1985; Ferguson 1989). While populations of LMCGs seem to follow basic dwarf galaxy photometric scaling laws, such as surface brightness with magnitude, there is relatively little detailed information about their intrinsic properties. To further understand these objects, and their origin, we have begun a series of papers to address these issues.

In Conselice, Gallagher and Wyse (2001a and 2002) (hereafter Papers I and II), we outlined several of the basic problems, and possible solutions, for understanding the origin of LMCGs. In Paper I we argued that Virgo cluster LMCGs as an aggregate population have dynamical properties and are spatially distributed in a way consistent with their being accreted after the development of the cluster core, as defined by the giant elliptical galaxies. This idea is supported by the high dispersion and non-Gaussian distributions of LMCG radial velocities and the large range in projected spatial positions of Virgo LMCGs. We also found that the velocity dispersion of the LMCGs exceeds that of the giant ellipticals in the cluster core by a factor consistent with the LMCGs being a weakly gravitationally bound and accreted component of the cluster.

In Paper I, we also argued that LMCGs cannot originate from galaxies born as field dEs or in groups because of the high LMCG to giant galaxy ratio in the Virgo cluster. If Virgo LMCGs originated solely from accreted field dwarfs we would expect the same giant-to-dwarf ratio in galaxy clusters as in the field. However, more LMCGs are found per giant cluster galaxy in nearby rich clusters (e.g., Thompson & Greggory 1993; Secker & Harris 1996). Paper I further argues that some Virgo LMCGs could originate from a more massive precursor population, such as disk galaxies, an idea also suggested in N-body models (e.g., Moore et al. 1998).

Paper II is the observational basis of the present paper, and in it we discuss methods for distinguishing different Perseus cluster galaxy populations. Paper II presented the observational results of a 173 arcmin² optical survey of the central region of the Perseus cluster ($v = 5366 \text{ km s}^{-1}$, $D = 77 \text{ Mpc}$). We argued, using the data in Paper II, that different galaxy populations can be separated from each other and background galaxies by their photometric and structural properties. We also demonstrated that for faint $M_B > -15$ Perseus cluster LMCGs, the universal elliptical galaxy color-magnitude relationship (CMR) breaks down. Previously (e.g., Bower, Lucey & Ellis 1992) it has been thought that the CMR was a linear relationship between magnitude and color. However, this is not the case

at faint, $M_B > -15$, magnitudes, due to the large range in colors found for faint cluster galaxies at a given magnitude (Paper II). Here we study this deviation from the color-magnitude relationship in detail to help determine the origin of LMCGs.

In this paper (Paper III of the series) we further explore in detail the properties of LMCGs in Perseus and in other nearby clusters, and compare their stellar-population characteristics to model predictions. In particular, we examine whether or not the dispersion in the Perseus cluster color-magnitude relationship for faint LMCGs with $M_B > -15$ can be reproduced in various models such as: formation of LMCGs from stripped spirals born in the field, self-enrichment induced by the confinement of metals in LMCG halos from the intracluster medium, and in situ formation out of intracluster gas. We also examine how these objects compare with predictions of various CDM models in which the mass and stellar populations of low-mass galaxies formed early, > 10 Gyrs ago (e.g., Dekel & Silk 1986), and had little, to no, active mass evolution or star formation since. Our general conclusion is that a significant proportion of LMCGs are consistent with originating from stripped higher mass galaxies accreted into clusters.

This paper is organized as follows: in §2 we discuss the observational data and selection criteria for LMCGs, presented in detail in Paper II, §3 gives an analysis of the early-type LMCG properties, while §4 compares these observations to various theories, and §5 gives a summary of our findings. We assume a Perseus distance of 77 Mpc throughout this paper, giving a scale of ~ 20 kpc per arcmin.

2. OBSERVATIONS AND DATA

2.1. *Observations*

All of the Perseus cluster imaging data used in this paper were taken with the WIYN 3.5m f/6.2 telescope at the Kitt Peak National Observatory. A detailed description of the data and a basic analysis of the photometric and structural properties of the cluster members, including the Perseus cluster luminosity function, was presented in Paper II. Briefly, the data come from two CCD cameras on WIYN, the S2kB and Mini-Mosaic. The S2kB is a thinned 2048² pixel charged coupled device (CCD). The scale of the images is 0.2'' pixel⁻¹, with a field of view 6.8' \times 6.8'. The S2kB imaging used to obtain deep B and R photometry took place on the nights on 1998 Nov 14 and 15 over an area of ~ 173 arcmin², in photometric conditions. The average seeing for all images over the two nights was 0.7''. Mini-Mosaic U-band data taken in 1999 December were also photometric with image fields 9.8' on a side. Only a fraction of the galaxies with BR photometry have reliable U-band data due to the small field covered with the Mini-Mosaic camera and defective areas on the mosaic chips due to imperfections and reflections. Our observed area was chosen to cover the central part of Perseus near NGC 1275, and along the linear array of large ellipticals to the west of NGC 1275 (see Paper II).

To calibrate the photometry, we fitted zero point offsets, airmass and color terms using UBR Landolt standard star photometry, acquired during each night (Paper II). Photometry for each galaxy was done in two ways. Magnitudes

representative of the entire galaxy were measured within an aperture, R_p , equal to three times an inverted Petrosian (1976) radius, or $R_p = 3 \times r(\eta = 0.5)$. We also measured core magnitudes and colors within the central $2''$ of each galaxy. We also correct the photometry for Galactic extinction, and for a slight k-correction. For more details on the sample selection and the data themselves, see Paper II. Monte Carlo simulations, and comparisons between the S2kB and Mini-Mosaic photometry, which is further discussed in Paper II, also argues that our photometry is reliable down to $B = 24$ or $M_B = -10.5$ at the adopted distance of the Perseus cluster.

2.2. Early-type LMCG Selection and Definition

This section briefly discusses how we are able to confidently identify LMCGs in the Perseus cluster from other cluster member and background systems in a reliable manner. See Paper II for a more detailed discussion and description of these issues. The summary of our selection criteria is the following:

- (i). Total $(B - R)_0$ colors of < 2 . Galaxies redder than this are almost always in the background. From stellar population synthesis models (Worley 1994), no normal passively evolving galaxy with metallicity $[\text{Fe}/\text{H}] = +0.5$ is redder than $(B - R)_0 \sim 2$ after an 18 Gyr initial burst of star formation. We further only investigate in detail Perseus LMCGs with magnitudes $M_B < -12.5$ to be more certain of cluster membership and to have very accurately measured photometric and structural parameters.
- (ii). Symmetric, round or elliptical shapes, without evidence for internal structures that might be due to star formation, spiral arms, or other internal features. Dwarf ellipticals/spheroidals appear this way, whereas background galaxies are often morphologically disturbed and can be identified as such in high resolution images (e.g., Conselice 2001).
- (iii). A central surface brightness in a $2''$ aperture fainter than $\mu_B = 24.0 \text{ mag arcsec}^{-2}$ and a non-centrally concentrated light profile that is close to exponential (see Paper II and §3.1). These are properties of nearby dwarf ellipticals and can be used to distinguish LMCGs from giant ellipticals and background systems.
- (iv) As discussed in Paper II, we also limit our study to objects that are detected above a 5σ confidence.

Figure 1 shows Harris R-band images of the LMCGs which we study in this paper and which constitute the galaxies that make up the low-luminosity scatter in the Perseus color-magnitude relationship (Paper II, Figure 2 & §3.4). We also somewhat arbitrarily separate LMCGs into blue and red types for discussion purposes. We define blue Perseus galaxies as those which are within $+2\sigma$ of the color-magnitude relationship scatter at $M_B = -17$ on the red side and everything bluer than this (see Conselice 2002). LMCGs which are $> 2\sigma$ redder than the CMR are denoted as red systems. Figure 3 shows the $(B - R)_0$ color histogram for Perseus LMCGs, down to $M_B = -11$, with the red and blue systems shaded differently (see Paper II).

In addition to Figure 1, which displays the R-band images of the 53 galaxies studied in this paper, Table 1 lists their positions, photometric and structural properties. For reference, the absolute magnitude M_B , $(B - R)_0$ color, and identification number are also listed in Table 1 and printed on Figure 1 for each galaxy.

3. RESULTS

3.1. Structures and Surface Photometry of the LMCGs

3.1.1. Previous Work

In Paper II we studied the basic photometric and structural properties of the Perseus LMCGs, including simple global morphological indexes such as asymmetry and concentration (Bershady, Jangren & Conselice 2000; Conselice, Bershady & Jangren 2000). We found that the concentration indexes and asymmetries of the LMCGs are consistent with dwarf elliptical-like objects. We also found a strong correlation between the central surface brightness and magnitudes of these objects, with the same relationship seen for nearby dwarfs (e.g., Binggeli & Cameron 1991). This suggests that all Perseus LMCGs are objects that would be classified, if nearby, as dwarf elliptical or spheroidals and are also thus likely cluster members. We go beyond this basic examination in this paper to determine the detailed structural properties of the Perseus LMCGs.

3.1.2. Surface Photometry

Previous studies have found that LMCGs in other clusters, as well as Local Group dSphs, have exponential profiles, while large ellipticals have steeper $r^{1/4}$ de Vaucouleur profiles and are found to be more rounder than LMCGs (Ryden & Terndrup 1994). What is the case for the Perseus LMCGs? To answer this, we perform surface photometry on all 53 early-type LMCGs and all the elliptical galaxies used in this paper. We fit elliptical isophotes to each galaxy image using the Fourier prescription of Jędrzejewski (1987), implemented by the ELLIPSE routine in STSDAS. We allow the ellipticity, position angle, and center to change while fitting. The general form of the Fourier decomposition of intensity distributions is

$$I(\phi, r) = I_0 + \sum_{i=1}^4 (a_i \sin(i\phi) + b_i \cos(i\phi)), \quad (1)$$

with a_i and b_i the fitted Fourier components, and ϕ the position angle at each fitted semi-major length r . For each surface brightness profile, $I(r)$, a general Sérsic profile of the form:

$$I(r) = I_0 \times \exp(-(r/r_0)^{(1/n)}), \quad (2)$$

is fit, where $I(r)$ is the intensity of an isophote at r , I_0 is the central intensity, and r_0 is the scale length. The value $n = 1$ is for pure exponential profiles, and $n = 4$ is the de Vaucouleurs profile that fits giant elliptical galaxies fairly well (e.g., Gavazzi et al. 2000). Table 1 lists the fitted profile parameters, n and r_0 , for each LMCG.

Figure 4 shows the detailed surface photometry and fitted parameters for the brightest, $M_B < -13.5$, early-type LMCGs in the Perseus cluster. The other LMCGs are generally too faint to obtain reliable measurements over a considerable range in radius. The first panel shows the surface brightness profiles for these galaxies and their best Sérsic profiles. The fits are generally good at the cores, but are sometimes poorer at larger radii.

The Sérsic fits for the galaxies listed in Table 1 are probably minimally affected by resolution. We determined this

by fitting isophotes and Sérsic profiles to stars in the various Perseus fields. Depending on the seeing of the images, the Sérsic index n for these stellar fits varies from 0.5 - 0.6, which is among the lowest values found for the LMCGs. The Sérsic radius r_0 is also very small $\sim 0.5''$, lower than all but a few of the LMCG values.

3.1.3. Isophotal Fits

The second panel in Figure 4 shows the fitted ellipticities, $\epsilon = (1 - a/b)$, for each isophote as a function of radius. The average ellipticity within $5''$ for each object is also printed in the second panel. In general, the ellipticities are constant with radius and most early-type LMCGs are fairly round with $\epsilon < 0.3$, with an average ellipticity within $5''$ for the objects in Figure 4 equal to 0.26 ± 0.16 (Table 1 also lists these $\langle \epsilon \rangle$ values). Other studies demonstrate that Virgo dwarf ellipticals are generally flatter than giant Es (Ryden & Terndrup 1994; Ryden et al. 1999). A few Perseus LMCGs have ellipticities that systematically increase at larger radii, i.e. are flatter in their outer parts. This does not significantly differ from the average ellipticity of giant ellipticals, $\langle \epsilon \rangle = 0.24 \pm 0.11$ (from data in Peletier et al. 1990 and Ryden et al. 1999).

The position angles (P.A.) of the isophotal fits (column 3 on Figure 4) are relatively constant with radius for all galaxies, indicating that isophotal twists are not common in Perseus LMCGs. The fourth column shows the a_4 component to the Fourier fits. The value of a_4 indicates the degree of deviation from purely elliptical isophotes, with $a_4 > 0$ indicating disk-like isophotes, and $a_4 < 0$ for boxy isophotes. The average a_4 for each galaxy is printed in the fourth panel of Figure 4, with nine LMCGs having $a_4 < 0$ and five with $a_4 > 0$. Most of the LMCGs have very small deviations from $a_4 = 0$, and only two LMCGs (31900.4+4129, 31941.7+4129) have large a_4 values. These a_4 values are roughly consistent with elliptical isophotes, with small variations, as is also seen for Virgo cluster dEs (Ryden et al. 1999).

3.1.4. Basic Interpretation

Most Local Group dwarf-ellipticals have observed exponential profiles, or King profiles (Faber & Lin 1983). The more general Sérsic profile is also found to provide a good fit to dE profiles, with most indexes at $n < 2$ (Davies et al. 1988; Binggeli & Cameron 1991). We find that the brightest galaxies we classified as giant ellipticals are well fit by de Vaucouleur profiles, although some of the fainter ellipticals appear to be better fit by an exponential (Figure 5).

Some previous studies found that more luminous Virgo dEs have surface brightness profiles with $n > 1$ (e.g., Young & Currie 1994; Durrell 1997). Table 1 and Figures 4 and 5 shows that most of the early-type LMCGs, chosen by morphology and color as cluster members, have nearly exponential profiles similar to dwarf elliptical galaxies. Only two LMCGs have higher n values near $n \sim 3$, although classified dEs in other clusters can have Sérsic indexes this high (Binggeli & Jerjen 1998).

We find no strong correlation between n and absolute magnitude for galaxies at $M_B > -17$ (Figure 5), contrasting with earlier claims for dE galaxies in the Virgo cluster (e.g., Young & Currie 1994; cf. Binggeli & Jerjen 1998). In

general it appears from Figure 5 that the brightest galaxies have the highest Sérsic indexes, n , although this correlation does not extend to fainter objects. It is however important to note that if there are very compact LMCGs with very high Sérsic n values, then we are liable to miss them in our morphological selection, as these objects will masquerade as stars or background ellipticals.

There is also no strong correlation between n and the $(B - R)_0$ color of the LMCGs (Figure 5). If these LMCGs were contaminated by smooth symmetric background galaxies (the only ones that would pass our morphological criteria), we would expect them to be red objects with steep, non-exponential, surface brightness profiles. No red object chosen as a LMCG was found to have this characteristic.

3.2. Internal Color Structures of LMCGs

A first impression of the Perseus LMCG images (Figure 1) is that some are nucleated; based solely on their structural appearance 17 (32%) have evidence of an excess central brightness. A critical observational test for determining the origin of early-type LMCGs, and these nuclei, is whether or not any color gradients exist within these galaxies. Pronounced radial color gradients are infrequently seen in dE galaxies (e.g., Caldwell & Bothun 1987; Vader et al. 1988; Cellone et al. 1994; Durrell 1997) and we find the same here. A lack of systematic color gradients in Perseus early-type LMCGs can be demonstrated in several ways, consistent with our later use of single stellar population synthesis models. First, color maps of bright dEs (Figure 6) reveal that these early-type LMCGs have no significant color gradients, or core colors that differ from those of the underlying light.

We further assessed the importance of radial color gradients by comparing the measured color of the core (central $2''$) for each dE to its total color, which includes the core regions. Figure 7 plots this relationship, where the solid squares are the color differences in the nucleated early-type LMCGs, and the open circles are the color differences in the non-nucleated objects. There is no significant color difference between the two different types, and there is no systematic trend between this color difference as a function of color. The color differences $(B - R)_0^{\text{tot}} - (B - R)_0^{\text{core}}$ and the 1σ variations are essentially the same for the two populations: -0.05 ± 0.16 for the nucleated LMCGs and -0.09 ± 0.17 for non-nucleated ones. This difference, 0.04 mag, is within our photometric color error (Paper II). The average colors ($\pm 1\sigma$) of the various components of these systems are also essentially the same with $\langle (B - R)_0 \rangle = 1.23 \pm 0.32$ for integrated LMCGs colors and $\langle (B - R)_0 \rangle = 1.29 \pm 0.33$ for their cores.

The lack of color gradients can also be demonstrated by measuring the difference in colors between the outer regions of the LMCGs, which does not include their cores, and their core colors. We apply this test by dividing galaxies into their inner parts ($r = 2''$) and the rest of the galaxies' light at $r > 2''$. The results of this comparison are shown by the solid triangles on Figure 7. Again, we find few Perseus LMCGs with significant color gradients between the centers and outer regions. The few LMCGs that do show significant differences could be galaxies with stellar populations at different ages and metallicities in their cores and envelopes. Some non-nucleated LMCGs

also have red cores, possibly the result of dust, very old stellar populations, or accreted globular clusters (Lotz et al. 2001). A few dEs in the Virgo cluster also contain blue nuclei, but the majority of nucleated objects have a central color similar to their host galaxies (Durrell 1997). Further observations, especially spectroscopy, will be necessary to determine if recent star formation could have produced the bluer nuclei.

3.3. Surface Densities and the Dwarf to Giant Ratio

The early-type dwarf to giant ratio (EDGR; Secker & Harris 1996; Phillipps et al. 1998) provides a quantitative measure of the form of the luminosity function, where galaxies are selected both by luminosity and morphology (Driver, Couch, & Phillipps 1998). In our 173 arcmin² survey of the Perseus cluster, we find 160 candidate early-type dwarf elliptical-like LMCGs with $M_B < -11$ (Paper II), giving a surface number density of ~ 1 arcmin⁻² or ~ 2000 early-type LMCGs Mpc⁻². The giant galaxy density is ~ 260 giants Mpc⁻². This gives an EDGR ratio of ~ 8 , which is lower than the Virgo or Coma value at the brighter magnitude limit $M_B = -12.5$ (e.g., Ferguson & Sandage 1991; Secker & Harris 1996). For LMCGs with $M_B < -12.5$, we find a surface density of ~ 0.5 arcmin⁻² or ~ 1000 Mpc⁻². This gives an EDGR ratio of ~ 4 , compared with the values 9.4 and 9.3 computed in the Coma and Virgo clusters (Secker & Harris 1996). Table 2 lists the values of the EDGR computed for Perseus and values from the Virgo and Coma clusters.

This result suggests that the EDGR ratio at the center of the Perseus cluster is lower than published values for the less dense Virgo cluster and integrated value for the Coma cluster (Ferguson & Sandage 1991; Secker & Harris 1996). The EDGR ratio was found by Ferguson & Sandage (1991) to correlate with galaxy group density, with denser groups displaying higher EDGRs. Other studies suggest an opposite trend for rich clusters, such that denser cluster regions contain lower EDGR ratios (Phillipps et al. 1998). A reduced surface density of LMCGs near the center of a rich cluster has been noted before (Thompson & Gregory 1993; Driver et al. 1998; Adami et al. 2000), and is possibly the result of galaxy destruction rather than initial conditions (Conselice 2002; §4.3). As pointed out by Thompson & Gregory (1993) in the Coma cluster, the processes creating LMCGs from stripping could become so efficient in the cores of rich clusters that many LMCGs are destroyed, or disrupted to the point where they are too faint to be detected.

3.4. The Color-Magnitude Relationship: Metallicity, Ages and Mass to Light Ratios

In Paper II we argued that for Perseus LMCGs fainter than $M_B \sim -15$, there is an increase in the scatter about the universal linear CMR established for giant ellipticals (Bower et al. 1992) (see Figure 2). This increase cannot be accounted for by photometric errors for systems more luminous than $M_B \sim -12.5$ (Paper II). Evidence that faint cluster dE galaxies scatter significantly from a linear CMR have been available for some time (e.g., Caldwell & Bothun 1987), but this has yet to be fully characterized, explained, or appreciated. To understand and characterize the galaxies that make up this scatter, we limit our

detailed analysis to the sample of early-type Perseus LMCGs with $M_B < -12.5$ listed in Table 1 and displayed in Figure 1.

The origin of the relationship between the colors and magnitudes of giant cluster elliptical galaxies has been debated since its initial characterization by Sandage & Visvanathan (1978), but it is now generally regarded as a relationship between a galaxy's mass (traced by its magnitude) and metallicity (traced by its color), with the stars in each galaxy at similarly old ages (Arimoto & Yoshii 1987; Bower et al. 1992). This idea is supported through studies of cluster galaxies at higher redshifts, where the scatter in the color-magnitude relationship remains low (Ellis et al. 1997; Stanford, Eisenhardt & Dickinson 1997). Metallicity as a driver of cluster galaxy colors is also an inherent aspect of various formation models (Arimoto & Yoshii 1987; Kauffmann & Charlot 1998). Below we demonstrate what our broadband UBR colors tell us about the nature of the stellar populations in LMCGs; specifically we demonstrate that the red colors of some LMCGs imply that they must be particularly metal enriched and that this enhanced enrichment is at least partially the cause of the large scatter of these galaxies from the color-magnitude relationship.

3.4.1. UBR Color-Color Plots: Constraining Ages and Metallicities

As we argue in §3.2 the internal colors of Perseus LMCGs are nearly homogeneous, such that we can to a first approximation consider their stars as single stellar populations (SSPs), to place constraints on their ages, metallicities and stellar masses. We investigate the properties of these stellar populations by comparing spectral energy distributions of LMCGs to the stellar population synthesis models of Worthey (1994), including the Padova isochrone library (Bertelli et al. 1994).

Figure 8 shows model $(U - B)_0 - (B - R)_0$ color-color tracks at three different ages ($\tau = 18, 12, 5$ Gyrs), plotted as a function of metallicity, with each panel showing a different age, along with the Perseus cluster data. All galaxies fall along, or close to these Worthey (1994) isochrones. If Perseus cluster galaxies contain stellar populations formed at roughly the same time, and are old, as clusters ellipticals are thought to be (e.g., Kuntschner & Davies 1998; Trager et al. 2000), then Perseus giant ellipticals have near solar metallicity stellar populations, while the Perseus LMCGs consist of stars with a range of lower metallicities.

Figure 9 shows corresponding color-color diagrams of models at three constant metallicities at different ages, with each panel containing a different constant metallicity model. From these figures it is clear that the colors of Perseus galaxies can be accounted for by a mix of various ages and metallicities. However, combining information from Figures 8 and 9 allows us to place some constraints on the ages and metallicities of the stellar populations that make up the Perseus LMCGs. Figure 9 shows that the $[Fe/H] = -0.5$, and any lower metallicity models, are unable to account for the reddest LMCGs, even if the ages of the stellar populations are ~ 18 Gyrs old, which is unlikely given the currently favored ~ 13 Gyr age of the universe (e.g., Ferreras, Melchiorri & Silk 2001). What this means is that the elliptical galaxies, and the reddest LMCGs with $(B - R)_0 > 1.4$, must have metallicities with

$[\text{Fe}/\text{H}] > -0.5$, unless these systems are dusty. If the stars in the reddest LMCGs are younger than ~ 12 Gyrs, and dust free, their metallicities must be even higher than $[\text{Fe}/\text{H}] = -0.5$. Due to an age-metallicity degeneracy in our broad-band colors this is the only constraint we can place on the metallicities and ages of the red LMCGs. We can place some constraints on the ages of the blue LMCGs by also using Figures 8 and 9. If the metallicities of the stellar populations in the bluest LMCGs, at $(B - R)_0 \sim 1$, are solar, $[\text{Fe}/\text{H}] = 0$, then their ages cannot be less than ~ 1 Gyr old. If these blue LMCGs have metallicities lower than solar, as seems likely given spectroscopic and photometric results demonstrating that blue LMCGs in other clusters are metal poor (e.g., Held & Mould 1994; Rakos et al. 2001), then their stars must be older than 1 Gyr.

Based on these arguments we will often assume that the $(B - R)_0$ colors of the LMCGs and giant ellipticals are representative of the metallicities of their stellar populations. This is not a new idea, as it is now generally thought that the colors of early-type galaxies in clusters are dominated by metallicity as opposed to age (e.g., Kuntschner & Davies 1998; Vazdekis et al. 2001). Prior observations through spectroscopy and narrow-band imaging also suggest that low-mass cluster galaxies have spectral signatures which are dominated by metallicity (e.g., Thuan 1985; Bothun & Mould 1988; Held & Mould 1994; Gorgas et al. 1997; Poggianti et al. 2001).

3.4.2. Mass-Metallicity Diagram and Mass to Light Ratios

Colors and magnitudes are observational quantities that we can convert into metallicity and mass given our assumptions in §3.4.1. By assuming that the $(B - R)_0$ colors of LMCGs and giant ellipticals trace metallicity in an old stellar population, we can find $[\text{Fe}/\text{H}]$ using the relationship from Harris (1996) for globular cluster systems, dichotomy remnants telescope

$$[\text{Fe}/\text{H}] = 3.44 \times (B - R)_0 - 5.35. \quad (3)$$

Transforming the magnitudes of objects into stellar masses (M_{stellar}) requires knowledge of the stellar mass to light ratio (M_{stellar}/L), which is a function of metallicity $[\text{Fe}/\text{H}]$ and age (τ),

$$\begin{aligned} M_{\text{stellar}} &= \frac{M_{\text{stellar}}}{L_B}([\text{Fe}/\text{H}], \tau) \times L_B \quad (4) \\ &= \frac{M_{\text{stellar}}}{L_B}([\text{Fe}/\text{H}], \tau) \times 10^{0.4(5.45 - M_B)}. \end{aligned}$$

By assuming that metallicity correlates with $(B - R)_0$ as given in equation (3), and by adopting an age (τ) for a stellar population, we can determine the relationship between $(B - R)_0$ and (M_{stellar}/L) . We take the value $\tau = 12$ Gyr as a representative age, although other ages do not give significantly different results in what follows. In this situation we can then write (M_{stellar}/L) as a power law of $(B - R)$ such that,

$$\frac{M_{\text{stellar}}}{L} \propto (B - R)_0^\kappa. \quad (5)$$

The relationship between (M_{stellar}/L) and $(B - R)_0$ is plotted in Figure 10 for $\tau = 8, 12$ and 14 Gyrs. At $\tau = 12$

Gyrs, $\kappa = 2.4$, which we use to calculate the stellar mass of each Perseus galaxy from its luminosity.

Using equations (3) and (4) we can create a metallicity-stellar mass diagram (Figure 11). Figure 11 shows that there are two stellar mass-metallicity sequences in the Perseus cluster. The blue (and now low-metallicity) LMCGs appear to blend naturally into the low-mass sequence of the higher mass elliptical galaxies. However, part of the LMCGs form a separate sequence that includes all the red LMCGs. Based solely on this diagram it is unclear what these two sequences imply for the formation and evolution of LMCGs, but it is a curious feature that any proposed LMCG origin scenario must explain.

4. THE ORIGIN OF LMCGS

4.1. Primordial Galaxies

A common theoretical presumption about low-mass galaxies, that we explore here, is that they are very old objects that originated in their present forms soon after the universe began, and possibly formed many of their stars before reionization at $z > 6.5$. Due to suppression of star formation caused by photoionization, star-formation in low mass galaxies with old stars should occur before reionization (Efstathiou 1992). The low luminosities, and hence likely low masses, of the early-type LMCGs suggests they fit the basic criteria for old galaxies, as they are found in dense regions, where hierarchical clustering models predict the oldest galaxies should be most abundant (e.g., White & Springel 2000).

The most generally accepted idea is that dwarf galaxies form from the gravitational collapse of baryonic material, possibly within dark matter halos, to produce the first generation of stars, with the remaining gas removed through supernova driven winds (e.g., Larson 1974; Dekel & Silk 1986; Silk, Wyse & Shields 1987; Ferrara & Tolstoy 2000). Predictions of detailed models show that dwarfs should be low metallicity systems with minor color gradients and less clustered than giant galaxies. Low metallicity is a general feature for the formation of low-mass galaxies in the early universe and we investigate this scenario here using the data described in §3.4 as well as other photometric results (Rakos et al. 2001) supplemented by dynamical data (Pedraza et al. 2002; Geha, Guhathakurta & van der Marel 2002) from other studies.

4.1.1. Internal Dynamics

In addition to predicting low metallicity systems, Dekel & Silk (1986) show, based on their model assumptions, how the internal velocities, σ , of low-mass galaxies should correlate with M_{total}/L ratios and luminosities (L), such that $M_{\text{total}}/L \sim L^{-0.37}$ and $\sigma \sim L^{0.19}$. We test these predictions with Virgo cluster LMCG internal velocity measurements made by Pedraza et al. (2002) and Geha et al. (2002). The relationship between M_V and internal velocity σ for these galaxies is shown in Figure 12. When we fit a power law to the relationship between σ and L , we find $\sigma \sim L^{0.31 \pm 0.05}$. The fitted exponent on L is $\sim 2\sigma$ away from the relationship predicted by Dekel & Silk. If we limit this fit to the fainter LMCGs at $M_V > -17$ we find $\sigma \sim L^{0.18 \pm 0.12}$, in good agreement with the models of Dekel & Silk.

After converting the sizes and velocity dispersions listed in Geha et al. (2002) into a pseudo-total mass using the relationship $M_{\text{total}} \approx \epsilon r_e \times \sigma^2$ we find that the M_{total}/L_V ratios for these Virgo LMCGs increases at lower luminosities. Fitting these two quantities together we find $M_{\text{total}}/L_V \sim L^{-0.25 \pm 0.24}$, broadly consistent with the Dekel & Silk slope predictions. In general, the above arguments suggest that the limited number of LMCGs with measured internal velocities are consistent with having evolved through a self-enrichment supernova wind outflow model, such as that proposed by Dekel & Silk, although these internal velocity samples are dominated only by a few bright LMCGs that tend to follow giant galaxy scaling relationships.

4.1.2. Stellar Populations

The most complete previous analysis of the stellar populations for a sizable population of LMCGs is that of Rakos et al. (2001), who estimated the ages and metallicities of 27 Fornax cluster dEs. Rakos et al. (2001) find that there is a broad age and metallicity distribution for this sample of Fornax dEs, with $[\text{Fe}/\text{H}]$ values ranging from -1.6 to -0.4 and ages from 9 to 12 Gyrs. From this, and the analysis in §3.4 where we conclude that red Perseus LMCGs can not be metal poor objects, it is difficult for all LMCGs to be primordial objects formed through the e.g., Dekel & Silk paradigm as we would expect to have a population of objects with homogeneously old and metal-poor stellar populations.

We also argue that not all LMCGs can form in a simple early collapse by directly comparing our data to CDM simulations that predict the properties of low-mass galaxies that all formed early in the universe. In Figure 13 we plot the color-magnitude diagram for the Perseus galaxies together with the luminosities and colors derived from predictions of low-mass galaxies from the Λ CDM hydrodynamic models of Nagamine et al. (2001) which are based on simple feedback mechanisms that do not take into account environmental effects. The high stellar mass objects in these simulations, with $M_{\text{stellar}} > 2 \times 10^9 h^{-1} M_\odot$, have a wide range in stellar ages and metals due to the hierarchical nature of their formation over time. The low-mass galaxies with $M_{\text{stellar}} < 2 \times 10^8 h^{-1} M_\odot$, on the other hand, experience only a brief epoch of star formation, with few new stars produced after the universe is ~ 2 Gyrs old. The conversion between metallicity and color for the Nagamine et al. (2001) simulated galaxies was achieved by adopting the Milky Way globular cluster-based relation (eq. 3).

There is a general agreement between the simulated Nagamine et al. (2001) and Perseus cluster galaxies properties, except at the faint and bright ends of the luminosity function. Bright Perseus galaxies are redder than the simulated points, and these Λ CDM models do not predict the observed population of red low-mass galaxies. It does, however, appear that the Λ CDM simulated objects, based on simple feedback mechanisms, can reproduce the blue LMCGs as metal-poor and old galaxies.

4.1.3. Extreme Dark Matter Halos

If the correlation of color and magnitude for bright galaxies represents a total mass-metallicity relationship and LMCGs are primordial and evolve through self-enrichment, then the fact that the color-magnitude relation breaks down could be the result of varying total mass

to light (M_{total}/L) ratios. That is, LMCGs could contain large amounts of dark matter. A very high total mass to light ratio could account for objects that have high metallicities, but appear faint, such as the red LMCGs in the supernova - self-enrichment scenario. That is, when metals are produced during star formation in these dark-matter-dominated galaxies they are not ejected into the intracluster medium due to the large gravitational potential of the galaxy, which essentially traps the metals long enough for subsequent generations of more metal rich stars to form.

The likelihood of this scenario can be examined using the color-magnitude and mass-metallicity relationships and properties of the red LMCGs. For LMCGs at $(B - R)_0 \sim 1.4$ to be at a similar location of the mass-metallicity/color-magnitude relationship as a brighter elliptical galaxy at the same color would require a total mass ~ 3 magnitudes higher, and thus a total mass to light ratio of $M_{\text{total}}/L \sim (2.5)^3 \times (M_{\text{total}}/L)_{\text{ellipticals}} \sim 15 \times (M_{\text{total}}/L)_{\text{ellipticals}}$. If we take the M_{total}/L values for ellipticals computed using galaxy-galaxy lensing by McKay et al. (2002), which are 425 ± 51 and 221 ± 26 in the Sloan Digitized Survey g' and r' bands, then the inferred LMCG $M_{\text{total}}/L \sim 6 \times 10^3$. This would require an enormous dark matter content and is about 10 times larger than any single galaxy M_{total}/L yet derived (e.g., Mateo 1998; Kleyna et al. 2002). However the intracluster medium in clusters could have stripped gas from low-mass halos early through ram-pressure (Gunn & Gott 1972) before significant star formation and without removing any dark matter, thereby producing a galaxy with a high M_{total}/L ratio.

The best way to determine if the LMCGs have these high mass to light ratios would be to measure their internal velocity dispersions out to a large radius (e.g., Kleyna et al. 2002). This type of information does not yet exist for any LMCGs. In fact, the only velocity dispersion measurements are those in the central parts of LMCGs (Pedraz et al. 2002; Geha et al. 2002) where dark matter is not found to be present in large amounts. Future observations through radial velocities of dE globular clusters or velocity dispersion profiles out to considerable distances are needed to determine total LMCG masses within a relatively large radius.

4.2. Non-Self Enrichment Stochastic Formation or Intracluster Medium Containment

The wide range in inferred metallicities for LMCGs suggests that a scenario different from the standard dark halo plus supernova wind blow out (Dekel & Silk 1986) is occurring during their formation. There are two alternative scenarios we discuss here which can potentially reproduce some observational properties of LMCGs. One is that some LMCGs have delayed formation times, possibly due to the ultraviolet background intensity at high redshifts that keeps the gas in LMCGs photoionized until $z \sim 1$ (Babul & Rees 1992). LMCGs would then form later out of enriched intracluster gas. This would be a formation scenario similar to, but not identical with, how globular clusters are formed (Fall & Rees 1986) in galaxies by the cooling of gas. The other possibility is that the intracluster medium is able to contain the metal rich ejecta of supernova, and subsequent star formation inside the halos of LMCGs uses this material to produce subsequent generations of metal-rich stellar populations.

The first scenario is very attractive as it mimics the same properties, and the lack of correlations between mass or luminosity with metallicity, as found for globular clusters (Djorgovski & Meylan 1994), and could explain the existence of the faint blue galaxies (Babul & Ferguson 1996). This scenario would require that gas in clusters be able to cool to form stars at different times. Alternatively, a similar method of LMCG formation could occur due to the outflowing material from the active nucleus at the center of NGC 1275 (Conselice et al. 2001b) interacting with the intracluster medium (e.g., Natarajan, Sigurdsson & Silk 1998).

The present day iron abundance in the Perseus cluster center is slightly lower than solar using the most optimistic estimates (e.g., Ulmer et al. 1987; Ponman et al. 1990; Molendi et al. 1998; Ezawa et al. 2001). If red LMCGs formed from gas in the intracluster medium with these abundances, this would explain their relatively high metallicities, assuming that the Fe abundance was put into place early from supernovae. This scenario would also naturally explain why, on average, LMCGs with younger stellar populations in Fornax have higher metallicities (Rakos et al. 2001).

A problem with this idea is that the material in the intracluster medium of the Perseus cluster must be able to cool and form stars without the presence of a dark matter halo and at different times. For this to occur dissipatively the cooling time must be shorter than the dynamical collapse time. The 10^7 K gas at the center of the Perseus cluster cools in a Hubble time, making it possible that some of this material goes into creating LMCGs at the cluster center. This leads to another problem in that LMCGs produced in this method would likely have radial velocities close to that of the intracluster gas and would be located towards the center of the cluster, where the gas cooling time is the lowest. Dynamical processes such as viralization within the cluster occur a Hubble time or longer, and thus these LMCGs would retain their birth velocities (see Paper I). The radial velocity and spatial distributions of LMCGs in clusters have larger dispersions than the centrally located giants (Paper I), making formation from the intracluster medium unlikely.

The possibility that the LMCGs do not lose their supernova products due to confinement by the intracluster medium would occur if the kinetic energy of supernova ejecta was not large enough to displace the intracluster gas surrounding the halo of a LMCG, and as such this material fell back into the LMCG where it was used in further generations of star formation (Babul & Rees 1992). A simple interpretation of this scenario would however suggest that the metallicities of the stellar populations in LMCGs should all be similarly metal-rich, which is contrary to the wide range of computed metallicities in Perseus (§3.4) and Fornax LMCGs (Rakos et al. 2001). There are also similar problems with this model reproducing the velocity structure of LMCGs (Paper I).

4.3. Mass Removal Processes

Another method of forming LMCGs is through the tidal stripping of higher-mass galaxies to form lower mass systems. The occurrence, strength, and importance of this process in clusters has been debated for many years (e.g., Spitzer 1958; Gallagher & Ostriker 1972; Richstone 1976;

Strom & Strom 1978; Merritt 1984; Aguilar & White 1986; Thompson & Gregory 1993; Lopez-Cruz 1997; Moore et al. 1998; Gnedin 1999; Conselice 2002) but is likely occurring (e.g., Conselice & Gallagher 1998, 1999).

As interactions should occur in clusters, it is possible that some galaxies in clusters, ones either present at its formation or ones that are later accreted, collide, or become stripped of enough mass to mimic the morphological and structural properties of LMCGs and dwarf ellipticals. Stripped gaseous material from disk galaxy mergers within the cluster could also develop and condense into low-mass galaxies as tidal dwarfs (e.g., Duc & Mirabel 1998). Candidate tidal dwarf galaxies in nearby clusters have observed high metallicities (Duc et al. 2001) that could evolve into red LMCGs. As tidal dwarfs are produced through low speed galaxy interactions, it is not clear if enough of these interactions would have occurred in the past to account for the red LMCG population seen in nearby clusters. Further observations and modeling of the production and survival of tidal dwarfs in a dense cluster-like environment are necessary to demonstrate the likelihood of this process creating substantial dwarfs, but it is one possible outcome of the interactions discussed here.

The strength of these interactions, and whether they arise from the overall mass distribution of the cluster (including dark matter) or from individual galaxies through high speed encounters depends on the fraction of cluster mass bound to galaxies, an uncertain and hard to measure quantity (Natarajan et al. 1998b). As such, we examine both of these dynamical mass stripping scenarios below.

4.3.1. Tidal Limitation

When a galaxy enters the core of a cluster it encounters intense gravitational tides from the cluster potential that can change the galaxy's size and mass. For galaxies whose orbits take them to within twice the core radius (R_c) there is a limiting relationship between the truncated tidal radius (r_T) and the internal velocity dispersion σ_g of the galaxy (Merritt 1984). The Perseus cluster has a core radius of $11'$ (Kent & Sargent 1983) and thus nearly all galaxies observed in our survey (Paper II) are within $2 \times R_c$, minus any projection effects. The ratio of the tidal radius of a galaxy, r_T , to the core radius of a cluster, R_c , is given by (Merritt 1984),

$$\frac{r_T}{R_c} = \frac{1}{2} \times \frac{\sigma_g}{\sigma_{cl}}, \quad (6)$$

where σ_{cl} is the observed velocity dispersion of the cluster, and $\sigma_{cl} = 1260 \text{ km s}^{-1}$ for Perseus (Kent & Sargent 1983). Using these values, we find that a tidally limited system has a ratio $r_T/\sigma_g = 0.13 \text{ kpc (km/s)}^{-1}$. While we do not have internal velocities for any of our Perseus LMCGs, we do have measured sizes which we can use to determine internal velocity dispersions by assuming that these objects are at the tidal limit. If we use $n \times r_e$ as the tidal radius (r_T) then we find that the internal velocity dispersion for Perseus LMCGs would vary from $\sim n \text{ km s}^{-1}$ to $8n \text{ km s}^{-1}$, and we would expect $n \sim 2 - 3$. The derived σ values are similar to, or just lower than, the measured internal velocity dispersions of nearby dwarf ellipticals (Mateo 1998) and for LMCGs in nearby clusters (Pedraz et al. 2002; Geha et al. 2002). In the Virgo

cluster, the computed tidal radii for the six galaxies with internal velocities studied by Geha et al. (2002) are larger by a factor of 5 - 7 than their effective radii, using the Virgo radial velocity given in Paper I and the core radii computed by Binggeli, Tammann & Sandage (1987). This implies that LMCGs in Virgo and Perseus could be tidally limited systems.

4.3.2. Collisional Stripping

If a large fraction of the mass inside a cluster is attached to galaxies then collisional interactions between galaxies will be the dominant method for removing mass. Most encounters between galaxies in clusters occur at high speeds, with $\delta v \sim \sigma_{\text{Cluster}} \gg \sigma_g$, which increases the internal energy in each system with a resulting gradual mass loss. In this situation the impulse approximation for the increase of internal energy of spherically symmetric systems can be used. This approximation is found to be reliable in many circumstances (e.g., Richstone 1976; Dekel et al. 1980; Aguilar & White 1985; Moore et al. 1998) and it is possible to parameterize analytically the mass loss rate in terms of the impact parameter, p , and the perturbed galaxy's half-light radius, r_e (e.g., Aguilar & White 1985)

The Aguilar & White (1985) formalism allows us to investigate the effects of mass-loss from high-speed galaxy encounters in the Perseus cluster core. A typical galaxy orbiting through Perseus will undergo impulsive interactions from all galaxies, but close encounters are more efficient at producing mass loss than distant ones. Without knowing the detailed orbital structure of every galaxy it is impossible to determine exactly the extent of individual interactions. Some estimates can be made by using averages, and understanding the limitations where impulse encounters are ineffective at removing mass. For a galaxy with an initial mass of $M = 10^{10} M_\odot$ and size $r_e = 3$ kpc interacting with a perturber of mass $M_p = 10^{11} M_\odot$, at a velocity of interaction $V = 1200 \text{ km s}^{-1}$ Aguilar & White (1985) gives a mass loss rate $\eta = \delta M/M = 0.1$ per interaction. After n interactions for every m cluster crossings, there are $q = n \times m$ total interactions, and the total mass of the galaxy after these interactions is, assuming that the change in mass produces no change in the interaction efficiency,

$$M_f = M_0(1 - \eta)^q. \quad (7)$$

Aguilar & White show (e.g., their Fig. 8) that the parameters we use in our calculations are in regime where galaxies should expand due to collisions. This implies that after one collision, the next one is likely to be at a somewhat smaller p/r_e just because r_e has increased. On the other hand, β could decrease because $(M \times r_e)^{1/2}$ increases in the regime that we are considering. The important factor is whether the post-collisional change in β or p is more important, which is not easy to calculate.

However, we can determine from Figure 5 in Aguilar & White (1985), that the β term is likely to dominate and the efficiency of mass-loss should decrease with each collision. We estimate a limit by assuming there is no change in the mean impact parameter, p . Thus we can obtain an upper bound to the mass loss after q collisions, but in reality the process would become self-limiting. The modeled collisions in Aguilar & White (1985) also take place in an

otherwise empty universe. Additional factors in real clusters, including perturbations from distant galaxies and the tidal field of the overall cluster (e.g., Merritt 1984) and the clumpiness of the cluster mass distribution (Gnedin 1999), may act to enhance these mass loss rates.

What is the expected mass loss evolution for a galaxy of initial mass $10^{10} M_\odot$ introduced in a Perseus like cluster as a function of time starting at $z = 1$, assuming the mass loss rate η remains constant? As a lower limit, we assume one $p=10$ interaction per core crossing with a crossing time of $\sim 0.5 \text{ Mpc} / 1200 \text{ pc/Myr} \sim 0.42 \text{ Gyrs}$. In this scenario $q = 2.4 \times t_{\text{clu}}$, where t_{clu} is the total time in Gyrs the galaxy has been in the cluster, or the time the cluster has had a fixed potential. Using the above description this galaxy will have a mass of $\sim 10^8 M_\odot$ at $z \sim 0$ (see also Conselice 2002). Thus, it is possible to produce LMCGs from high mass galaxies through collisional stripping (see also Moore et al. 1998).

4.3.3. Stellar Populations and Properties

Given the above discussion we investigate, in this section, the idea that LMCGs are remnants of accreted disk galaxies. In Paper I we argued that LMCGs in the Virgo cluster have kinematic and spatial signatures suggesting these galaxies, or their progenitors, were accreted in the last few Gyrs. Depending on the details of the interactions, accreted galaxies could lose $>90\%$, to all, of their initial mass after undergoing these tidal processes. The effectiveness of mass loss could also be increased by gas removal processes in unevolved disk galaxies. If mass loss occurred in the past, it is a natural explanation for the production of some LMCGs from more massive, and hence redder progenitors.

Since many bulges, and the centers of other high mass galaxies, have dominant metal-rich populations (e.g., Wyse, Gilmore & Franx 1997) and observations of LMCGs in various nearby clusters also reveal metal-rich signatures and similarly red colors (§3.4 and e.g., Bothun & Mould 1988; Held & Mould 1994; Rakos et al. 2001), it is possible that Perseus LMCGs are consistent with being the remnants of more massive progenitors whose outer parts have been stripped away.

We can further examine the likelihood of collisional and tidal limitation scenarios by examining the Sérsic scale length (r_0) of the LMCGs as a function of color (Figure 14). The fact that the red LMCGs (triangles) all have small effective radii is another indication that at least the red LMCGs have undergone some type of tidal limitation process, or collisional removal of mass. These red LMCGs also have a higher surface brightness than the bluer LMCGs at a given luminosity (Paper II), further suggesting that the red LMCGs are stripped down components of larger galaxies.

By comparing the colors of bulges of 257 Sbc galaxies from Gadotti & dos Anjos (2001) and Peletier & Balcells (1997) to the colors of LMCGs we can test if there is a relationship between bulges and LMCGs by comparing the distribution of their colors. Figure 15 is the histogram of $(B - R)_0$ colors from these two studies. Gadotti & dos Anjos give $(B - V)_0$ and $(U - B)_0$ bulge colors which we convert into $(B - R)_0$ colors by determining the relationship between $(B - V)_0$ and $(B - R)_0$ based on Worthey (1994) population synthesis models. The conversion we

use assumes that $(B - V)_0$ color is the result of different ages at a constant metallicity of $[\text{Fe}/\text{H}] = -0.2$, but the results do not change significantly if we assume colors are the result of different metallicities. The distribution of bulge colors from Gadotti & dos Anjos (2001) is shown in Figure 15 as an open histogram while the bulge colors from early type galaxies from Peletier & Balcells (1997) are shown as the shaded histogram. The distribution of bulge colors is similar to the color distribution of the LMCGs (Figure 3).

A prediction from the tidal stripping scenario is that a substantial number of intracluster stars should exist. These would be the bulk of the stars, $> 99\%$, that were lost to create each stripped LMCGs. The existence of these intracluster stars is suggested through several pieces of observational evidence. Between 25% - 50% of the light from galaxy clusters originates in intracluster regions (e.g., Melnick, White & Hoessel 1977; Bernstein et al. 1995; Feldmeier et al. 2002). Evolved stars are also found in the intracluster medium (e.g., Ferguson, Tanvir & von Hippel 1998; Feldmeier, Ciardullo & Jacoby 1998; Arnaboldi et al. 2000; Durrell et al. 2002) that could be remnants of stripped material from LMCG precursors. There are also several examples of debris arcs of diffuse light (Trentham & Mobasher 1998; Gregg & West 1998; Calzeneo-Roldan et al. 2000) and red distorted galaxies in clusters (e.g., Conselice & Gallagher 1999) that could be contemporary examples of this tidal stripping process at work.

We can place further limits on tidal stripping occurring in clusters by using the results of intracluster light and planetary nebula surveys (Arnaboldi et al. 2002; Durrell et al. 2002). The metallicities of red giant branch and asymptotic giant branch stars found in the Virgo cluster intracluster medium are found to be $-0.8 < [\text{Fe}/\text{H}] < -0.2$, consistent with having originated in moderate luminosity galaxies (Durrell et al. 2002). The total luminosity of the intracluster light within 2° of M87 is $\sim 2 \times 10^{11} \text{ L}_\odot$ (Durrell et al. 2002), and if this material originates from tidally stripped objects whose remnants we now tentatively identify as LMCGs, we can compute how much material, on average, each LMCG must have lost. Using the Virgo Cluster Catalog from Binggeli, Sandage & Tammann (1985) we can calculate the number of classified dwarf ellipticals, nucleated dwarf ellipticals and S0s within 2° of M87. We only consider these three populations as they are the only types in Virgo that have kinematic evidence of past accretion (Paper I).

There are 170 dEs, 148 dE,Ns and 14 S0s within this radius. On average, if all the dEs and dE,Ns are remnants of stripped galaxies then $\sim 0.6 \times 10^9 \text{ L}_\odot$ was lost by each object. This number remains unchanged if we consider S0s to have lost a similar amount of mass. If we consider only the dEs or dE,Ns as remnants of this process then $1.1 \times 10^9 \text{ L}_\odot$ and $1.3 \times 10^9 \text{ L}_\odot$ was lost by each dE and dE,N, respectively. This is enough material to suggest that each LMCGs could have been a moderate sized disk galaxies in the past.

5. SUMMARY AND CONCLUSIONS

In this paper, we study the photometric properties of a complete sample of candidate early-type low-mass cluster galaxies (LMCGs) in the Perseus cluster to place constraints on their origin. Our major findings can be summarized as:

I. Dwarf elliptical-like LMCGs at $-12.5 > M_B > -15$ scatter from the color-magnitude relationship extrapolated from giant elliptical galaxies, although the ‘mean’ LMCG still follows the color-magnitude relationship. There are individual LMCGs that are both too blue and too red for their magnitudes. If we interpret these colors as indications of metallicity, then there exists a range of stellar population metallicities in early-type LMCGs in Perseus, similar to the broad metallicity distributions inferred for dwarfs in other galaxy clusters (Rakos et al. 2001; Poggianti 2001). A range of ages could also be present; this is not ruled out by our data, and has in fact been concluded by others (e.g., Held & Mould 1994; Rakos et al. 2001).

II. Using photometric and kinematic results from this, and other studies, we show that some Perseus LMCGs have colors and population color dispersions that are generally consistent with models that include early star formation plus feedback (Larson 1974), including those based on CDM cosmological scenarios (Dekel & Silk 1986; Nagamine et al. 2001). Trends between velocity dispersion, luminosity and total mass to light ratios for LMCGs at $M_B > -17$ are consistent with the self-enrichment supernova model for low-mass galaxies formation (Dekel & Silk 1986), although dynamical measurements have only been completed for a few galaxies in Virgo. Because of their possible low metallicities and old stellar population ages, some LMCGs are potentially among the first galaxies to form stars in the universe.

III. The large number of LMCGs that are redder than the mean color-magnitude relationship cannot originate from a simple self-enrichment evolutionary path of initial formation from collapse plus later feedback. Our analysis and others (e.g., Rakos et al. 2001) reveal that these redder LMCGs probably contain stellar populations with high metallicities, up to solar. These objects therefore must have formed in a manner fundamentally different than the majority of Local Group low mass galaxies. We identify four possible scenarios for explaining these systems: containment of metals in a halo by the intracluster medium, delayed formation out of intracluster gas with non-self enrichment (e.g., like globular clusters), very massive dark halos with $M_{\text{total}}/L_B \sim 6 \times 10^3$, and as the remnants of stripped spiral galaxies. Various observational evidence concerning LMCGs themselves, and intracluster light, suggests that the most likely of these scenarios is that the redder LMCGs are produced by tidal stripping.

Another more unlikely formation scenario, we have not discussed, is that initial mass functions for stars in LMCGs have extremely low upper mass limits or very steep faint end slopes. This would allow these galaxies to contain a excess amount of low-mass stars which would result in their observed red colors. However, there is no obvious physical mechanisms that would result in this situation and we do not consider this scenario likely. To further suggest which of the above scenarios is occurring to produce LMCGs will require further observations. We argue however that no single explanation can likely account for all LMCGs, and that the formation mechanisms for low-mass galaxies in clusters is fundamentally different than that for low-mass galaxies in groups.

We thank the staff of WIYN and NOAO for their support in obtaining the observations presented here. We also thank Kentaro Nagamine, Renyue Cen and Jeremiah Os-

triker for their Λ CDM model results. We especially thank Linda Sparke whose carefully reading and criticisms of a previous version of this paper resulted in a nearly complete rewrite. This research was supported in part by the National Science Foundation (NSF) through grants AST-9803018 to the University of Wisconsin-Madison and AST-9804706 to Johns Hopkins University. CJC acknowledges support from a Grant-In-Aid of Research from Sigma Xi and the National Academy of Sciences (NAS) as well as a Graduate Student Researchers Program (GSRP) Fellowship from NASA and the Graduate Student Program at the Space Telescope Science Institute (STScI).

REFERENCES

Adami, C., Ulmer, M.P., Durret, F., Nichol, R.C., Mazure, A., Holden, B.P., Romer, A.K., & Savine, C. 2000, *A&A*, 353, 930

Aguilar, L.A., & White, S.D.M. 1985, *ApJ*, 295, 374

Arimoto, N., & Yoshii, Y. 1987, *A&A*, 173, 23

Arnaboldi, M., et al. 2001, *AJ*, in press, preprint:astro-ph/0110522

Babul, A., & Rees, M.J. 1992, *MNRAS*, 255, 346

Babul, A., & Ferguson, H.C. 1996, *ApJ*, 458, 100

Balcells, M., & Peletier, R.F. 1994, *AJ*, 107, 135

Bernstein, G.M., Nichol, R.C., Tyson, J.A., Ulmer, M.P., & Wittman, D. 1995, *AJ*, 110, 1507

Bershady, M.A., Jangren, A., & Conselice, C.J. 2000, *AJ*, 119, 2645

Bertelli, G., Bressan, A., Chiosi, C., Fagotto, F., Nasi, E. 1994, *A&AS*, 106, 275

Binggeli, B., Sandage, A., & Tammann, G.A. 1985, *AJ*, 90, 1681

Binggeli, B., Tammann, G., & Sandage, A. 1987, *AJ*, 94, 251

Binggeli, B., & Cameron, L.M. 1991, *A&A*, 252, 27

Binggeli, B., & Jerjen, H. 1998, *A&A*, 333, 17

Bothun, G.D., & Caldwell, C.N. 1984, *ApJ*, 270, 41L

Bothun, G.D., Mould, J.R., Wirth, A., & Caldwell, N. 1985, *AJ*, 90, 697

Bothun, G.D., & Mould, J.R. 1988, *ApJ*, 324, 123

Bower, R.G., Lucey, J., & Ellis, R.S. 1992, *MNRAS*, 254, 601

Calcareo-Roldan, C., Moore, B., Bland-Hawthorn, J., Malin, D., & Sadler, E. 2000, *MNRAS*, 314, 324

Caldwell, N., & Bothun, G.D. 1987, *AJ*, 94, 1126

Cellone, S.A., Forte, J.C., & Geisler, D. 1994, *ApJS*, 93, 397

Cen, R. 2001, *ApJ*, 546, 77L

Conselice, C.J., & Gallagher, J.S. 1998, *MNRAS*, 297, 34L

Conselice, C.J., & Gallagher, J.S. 1999, *AJ*, 117, 75

Conselice, C.J., Gallagher, J.S., & Wyse, R.F.G. 2001a, *ApJ*, 559, 791 (Paper I)

Conselice, C.J., Gallagher, J.S., & Wyse, R.F.G. 2001b, *AJ*, 122, 2281

Conselice, C.J., Gallagher, J.S., & Wyse, R.F.G. 2002, *AJ*, 123, 2246 (Paper II)

Conselice, C.J. 2002, *ApJ*, 573, 5L

Davies, J., Phillips, S., Cawson, M., Disney, M., & Kibblewhite, E. 1988, *MNRAS*, 232, 239

Dekel, A., Lecar, M., & Shaham, J. 1980, *ApJ*, 241, 946

Dekel, A., & Silk, J. 1986, *ApJ*, 303, 39

de Propris, R., Pritchett, C.J., Harris, W.E., & McClure, R.D. 1995, *ApJ*, 450, 534

Djorgovski, S., & Meylan, G. 1994, *AJ*, 108, 1292

Driver, S.P., Couch, W.J., & Phillipps, S. 1998, *MNRAS*, 301, 369

Duc, P.-A., & Mirabel, I.F. 1998, *A&A*, 333, 813

Duc, P.-A., Cayatte, V., Balkowski, C., Thuan, T.X., Papaderos, P., & van Driel, W. 2001, *A&A*, 369, 763

Durrell, P.R. 1997, *AJ*, 113, 531

Durrell, P.R., Ciardullo, R., Feldmeier, J.J., Jacoby, G.H., & Sigurdsson, S. 2002, *ApJ*, 570, 119

Efstathiou, G. 1992, *MNRAS*, 256, 43

Ellis, R.S., Smail, I., Dressler, A., Couch, W.C., Oemler, A.O., Butcher, H., & Sharpless, R.M. 1997, *ApJ*, 483, 582

Ezawa, H., et al. 2001, *PASJ*, 53, 595

Fall, S.M., & Rees, M.J. 1985, *ApJ*, 298, 18

Feldmeier, J.J., Ciardullo, R., & Jacoby, G.H. 1998, *ApJ*, 503, 109

Feldmeier, J.J., Mihos, J.C., Morrison, H.L., Rodney, S.A., & Harding, P. 2002, preprint astro-ph/0204467

Ferrara, A., & Tolstoy, E. 2000, *MNRAS*, 313, 291

Ferreras, I., Melchiorri, A., Silk, J. 2001, *MNRAS*, 327, 47

Ferguson, H.C., & Binggeli, B. 1994, *A&ARv*, 6, 67

Ferguson, H.C. 1989, *AJ*, 98, 367

Ferguson, H.C., & Sandage, A. 1991, *AJ*, 101, 765

Ferguson, H.C., Tanvir, N.R., & von Hippel, T. 1998, *Nature*, 391, 461

Ferrara, A., & Tolstoy, E. 2000, *MNRAS*, 313, 291

Gadotti, D.A., & dos Anjos, S. 2001, *AJ*, 122, 1298

Gallagher, J.S., & Ostriker, J.P. 1972, *AJ*, 77, 288

Gallagher, J.S., & Hunter, D.A. 1986, *AJ*, 92, 557

Gavazzi, G., Franzetti, P., Scodéglio, M., Boselli, A., & Pierini, D. 2000, *A&A*, 361, 863

Geha, M., Guhathakurta, P., & van der Marel, R.P. 2002, preprint, astro-ph/0206153

Gorgas, J., Pedraz, S., Guzman, R., Cardiel, N., & Gonzalez, J.J. 1997, *ApJ*, 481, 19L

Gregg, M.D., & West, M.J. 1998, *Nature*, 396, 549

Gunn, J.E., & Gott, J.R. 1972, *ApJ*, 176, 105

Harris, W.E. 1996, *AJ*, 112, 1487

Held, E.V., & Mould, J.R. 1994, *AJ*, 107, 1307

Hodge, P.W. 1959, *PASP*, 71, 28

Hodge, P.W. 1960, *PASP*, 72, 188

Hodge, P.W. 1965, *AJ*, 70, 559

Ibata, R.A., Gilmore, G., & Irwin, M.J. 1995, *MNRAS*, 277, 78

Ichikawa, S.-I., Wakamatsu, K.-I., & Okamura, S. 1986, *ApJS*, 60, 475

Kent, S.M., & Sargent, W.L.W. 1983, *AJ*, 88, 697

Kepner, J.V., Babul, R., & Spergel, D.N. 1997, *ApJ*, 487, 61

Kleyna, J.T., Wilkinson, M.I., Evans, N.W., Gilmore, G., Frayn, C. 2002, *MNRAS*, 330, 729

Kuntschner, H., & Davies, R.L. 1998, *MNRAS*, 295, 29L

Lake, G. 1990, *ApJ*, 356, 43L

Larson, R.B. 1974, *MNRAS*, 169, 229L

Lotz, J., Telford, R., Ferguson, H.C., Miller, B.W., Stiavelli, M., & Mack, J. 2001, *ApJ*, 552, 572L

Mao, S., & Mo, H.J. 1998, *MNRAS*, 296, 847

Mateo, M.L. 1998, *ARA&A*, 36, 435

McKay, T.A., et al. 2002, preprint astro-ph/0108013

Melnick, J., Hoessel, J., & White, S.D.M. 1977, *MNRAS*, 180, 207

Merritt, D. 1984, *ApJ*, 276, 26

Mobasher, B., et al. 2001, *ApJS* in press, preprint: astro-ph/0107385

Molendi, S., et al. 1998, *ApJ*, 499, 608

Moore, B., Lake, G., & Katz, N. 1998, *ApJ*, 495, 139

Moore, B., Quinn, T., Governato, F., Stadel, J., & Lake, G. 1999, *MNRAS*, 310, 1147

Moore, B., Lake, G., Quinn, T., & Stadel, J. 1999, *MNRAS*, 304, 465

Nagamine, K., Fukugita, M., Cen, R., & Ostriker, J.P. 2001, *ApJ*, in press

Natarajan, P., Sigurdsson, S., & Silk, J. 1998, *MNRAS*, 298, 577

Natarajan, P., Kneib, J.-P., Smail, I., & Ellis, R.S. 1998b, *ApJ*, 499, 600

Pedraz, S., Gorgas, J., Cardiel, N., Sanchez-Blazquez, P., & Guzman, R. 2002, *MNRAS*, 332, 59L

Peletier, R.F., & Balcells, M. 1997, *New Astronomy*, 1, 349

Peletier, R.F., Davies, R.L., Illingworth, G.D., Davis, L.E., & Cawson, M. 1990, *AJ*, 100, 1091

Peterson, R.C., & Caldwell, N. 1993, *AJ*, 105, 1411

Petrosian, V. 1976, *ApJ*, 210, 53L

Phillipps, S., Driver, S.P., Couch, W.J., & Smith, R.M. 1998, *ApJ*, 498, 119L

Poggianti, B.M., et al. 2001, *ApJ*, in press, preprint: astro-ph/0107158

Ponman, T.J., Bertram, D., Church, M.J., Eyles, C.J., Watt, M.P., Skinner, G.K., & Willmore, A.P. 1990, *Nature*, 347, 450

Rakos, K., Schombert, J., Maitzen, H.M., Prugovecki, S., & Odell, A. 2001, *AJ*, 121, 1974

Reeves, G. 1956, *AJ*, 61, 69

Reeves, G. 1977, *AJ*, 89, 620

Richtstone, D.O. 1976, *ApJ*, 204, 642

Ryden, B.S., & Terndrup, D.M. 1994, *ApJ*, 425, 43

Ryden, B.S., Terndrup, D.M., Pogge, R.W., & Lauer, T.R. 1999, *ApJ*, 517, 650

Sandage, A., & Visvanathan, N. 1978, *ApJ*, 223, 707

Secker, J., & Harris, W.E. 1996, *ApJ*, 469, 623

Secker, J., Harris, W.E., & Plummer, J.D. 1997, *PASP*, 109, 1377

Silk, J., Wyse, R.F.G., & Shields, G.A. 1987, *ApJ*, 322, 59L

Stanford, S.A., Eisenhardt, P.R., Dickinson, M. 1998, *ApJ*, 492, 461

Strom, S.E., & Strom, K.E. 1978, *ApJ*, 225, 93L

Thompson, L.A., & Gregory, S.A. 1993, *AJ*, 106, 2197

Thuan, T.X. 1985, *ApJ*, 299, 881

Trager, S.C., Faber, S.M., Worthey, G., & Gonzalez, J.J. 2000, *AJ*, 119, 1645

Trentham, N., & Mobasher, B. 1998, *MNRAS*, 293, 53

Ulmer, M.P., Crudace, R.G., Fritz, G.G., Synder, W.A., & Fenimore, E.E. 1987, *ApJ*, 319, 118

Vader, J.P., Vigroux, L., Lachieze-Rey, M., & Souviron, J. 1988, *A&A*, 203, 217

van den Bergh, S. 2000, “The galaxies of the Local Group”, Cambridge Astrophysics Series Series, 35, Cambridge University Press

Vazdekis, A., Kuntschner, H., Davies, R.L., Arimoto, N., Nakamura, O., & Peletier, R. 2001, *ApJ*, 551, 127L

White, S.D.M., & Rees, M.J. 1978, *MNRAS*, 183, 341

White, S.D.M., & Frenk, C.S. 1991, *ApJ*, 379, 52

White, S.D.M., & Springel, V. 2000, in “The First Stars”, MPA/ESO Workshop, ed. A. Weiss, T. G. Abel, V. Hill, Springer, p.327

Worthey, G. 1994, *ApJS*, 95, 107

Wyse, R.F.G., Gilmore, G., & Franx, M. 1997, *ARA&A*, 35, 637

Young, C.K., & Currie, M.J. 1994, *MNRAS*, 268, 11L

TABLE 1
CANDIDATE LOW-MASS GALAXIES IN THE PERSEUS CLUSTER CORE

Number	R.A. (J2000)	Dec. (J2000)	M _B	(B-R)	Nucleation	r ₀	n	< ϵ >
1	3 18 53.5	+41 31 50.1	20.54±0.02	0.91±0.05	N	2.5±0.1	0.4±0.2	...
2	3 18 53.8	+41 32 52.3	20.01±0.01	1.14±0.05	N	2.3±0.1	0.7±0.1	0.41
3	3 18 54.9	+41 25 55.3	21.61±0.04	1.80±0.05	N	1.2±0.1	0.8±0.2	...
4	3 18 55.7	+41 25 54.4	20.76±0.03	1.44±0.04	Y	1.4±0.0	0.4±0.2	...
5	3 18 55.8	+41 23 41.3	21.46±0.03	1.55±0.05	N	1.6±0.0	0.4±0.3	...
6	3 18 57.8	+41 24 57.6	20.06±0.01	1.22±0.04	N	2.2±0.1	0.9±0.1	0.42
7	3 18 59.5	+41 31 18.9	21.39±0.04	0.89±0.07	N
8	3 18 59.7	+41 26 40.0	19.71±0.01	1.32±0.04	Y	2.3±0.1	0.8±0.1	0.11
9	3 18 59.8	+41 30 37.1	21.34±0.02	0.75±0.05	N	2.7±0.1	0.9±0.1	...
10	3 19 00.4	+41 29 02.4	20.26±0.02	1.29±0.05	Y	1.6±0.2	0.9±0.1	0.15
11	3 19 03.5	+41 35 13.6	20.21±0.02	1.09±0.05	N	2.9±0.3	1.3±0.2	0.43
12	3 19 04.2	+41 35 20.6	20.95±0.02	1.15±0.04	N	0.8±0.2	0.6±0.5	...
13	3 19 04.7	+41 32 24.6	21.50±0.02	1.95±0.05	N	1.3±0.0	0.6±0.1	...
14	3 19 05.2	+41 25 07.0	21.87±0.04	1.58±0.06	Y	0.7±0.0	0.8±0.1	0.39
15	3 19 05.2	+41 34 48.1	20.37±0.02	1.09±0.05	Y	1.5±0.7	1.3±0.5	...
16	3 19 06.0	+41 26 18.7	19.78±0.02	1.26±0.05	Y	0.3±0.3	2.0±0.2	0.05
17	3 19 06.8	+41 26 40.8	20.86±0.05	1.70±0.06	Y	0.9±0.1	3.2±0.1	...
18	3 19 09.1	+41 32 41.7	21.57±0.02	1.01±0.04	N	2.0±0.0	0.7±0.1	...
19	3 19 09.5	+41 31 30.9	20.59±0.01	0.91±0.04	N	1.2±0.1	0.9±0.1	...
20	3 19 10.4	+41 29 37.0	19.27±0.01	1.27±0.04	Y	1.2±0.3	1.2±0.2	0.08
21	3 19 12.7	+41 30 37.7	21.61±0.04	1.00±0.07	N	4.2±0.5	1.6±0.1	...
22	3 19 13.0	+41 34 51.8	20.10±0.01	1.72±0.04	Y	1.2±0.0	0.7±0.1	0.20
23	3 19 14.9	+41 30 27.1	21.77±0.06	0.85±0.11	N	0.2±0.7	3.1±0.2	...
24	3 19 15.1	+41 28 56.6	21.40±0.05	1.12±0.04	N	1.4±0.1	0.8±0.2	...
25	3 19 15.9	+41 30 20.3	21.89±0.05	1.11±0.08	N	1.1±0.1	0.9±0.2	...
26	3 19 17.3	+41 34 54.5	21.97±0.04	1.63±0.06	N	1.0±0.2	0.8±0.4	...
27	3 19 17.6	+41 29 57.7	21.40±0.05	1.64±0.05	N	0.9±0.3	1.3±0.3	...
28	3 19 18.0	+41 24 25.3	21.62±0.03	1.25±0.05	N	0.7±0.0	0.6±0.2	...
29	3 19 18.8	+41 26 32.4	20.94±0.03	1.02±0.06	Y	0.5±0.2	1.5±0.1	...
30	3 19 20.1	+41 24 06.6	21.34±0.04	1.57±0.06	Y	1.1±0.3	0.7±0.9	...
31	3 19 21.2	+41 28 42.5	20.77±0.03	1.40±0.06	N	3.3±0.1	1.4±0.1	...
32	3 19 22.1	+41 24 27.2	20.15±0.01	1.16±0.04	N	2.7±0.0	0.8±0.1	0.52
33	3 19 22.4	+41 24 04.2	21.75±0.05	1.90±0.07	N
34	3 19 24.6	+41 25 53.4	21.75±0.05	1.29±0.06	N	0.9±0.1	1.0±0.1	...
35	3 19 24.7	+41 24 36.3	21.90±0.07	1.65±0.08	N	1.5±0.0	0.5±0.2	...
36	3 19 24.7	+41 25 52.6	21.80±0.03	1.48±0.05	N	1.1±0.0	0.6±0.2	...
37	3 19 26.9	+41 33 05.1	20.74±0.03	1.43±0.06	Y	1.5±0.4	0.4±1.3	...
38	3 19 27.1	+41 27 16.1	18.48±0.01	1.43±0.04	Y	1.6±0.0	1.1±0.0	0.11
39	3 19 31.4	+41 26 28.7	18.72±0.01	1.39±0.04	Y	1.5±0.1	1.2±0.1	0.34
40	3 19 31.7	+41 31 21.3	19.30±0.01	1.24±0.04	Y	2.3±0.1	1.0±0.1	0.20
41	3 19 33.5	+41 24 39.4	21.76±0.08	1.55±0.10	N	0.8±1.5	1.8±0.9	...
42	3 19 36.1	+41 32 47.4	21.82±0.03	1.01±0.05	N
43	3 19 38.6	+41 33 46.1	21.92±0.03	1.03±0.05	N	0.8±0.0	0.5±0.1	...
44	3 19 39.7	+41 26 39.1	21.05±0.02	1.21±0.05	N	0.6±0.0	0.9±0.1	...
45	3 19 41.7	+41 29 17.0	18.72±0.01	1.42±0.04	Y	1.9±0.1	1.1±0.1	0.19
46	3 19 42.3	+41 34 16.6	20.67±0.02	1.04±0.05	Y	1.9±0.1	0.6±0.4	...
47	3 19 43.5	+41 28 52.9	20.87±0.02	1.24±0.05	N	3.0±0.1	0.9±0.0	...
48	3 19 45.7	+41 32 18.0	21.56±0.05	0.44±0.11	N	1.5±0.1	0.9±0.1	...
49	3 19 46.1	+41 24 51.2	21.43±0.03	1.41±0.05	N	0.9±0.0	0.8±0.1	...
50	3 19 55.4	+41 25 04.4	21.06±0.02	1.87±0.05	N
51	3 19 56.1	+41 29 09.4	20.71±0.01	1.42±0.04	N	0.7±0.0	0.7±0.1	...
52	3 19 56.1	+41 32 38.7	21.31±0.02	1.87±0.05	N	0.6±0.1	1.0±0.1	...
53	3 19 58.5	+41 31 02.0	21.86±0.03	1.00±0.06	N	0.7±0.0	0.7±0.1	...

TABLE 2
EARLY-TYPE DWARF TO GIANT GALAXY RATIOS (EDGR)

M_B limit	N(LMCG) Perseus	Perseus EDGR	Coma ^a EDGR	Virgo ^b EDGR
-15.5	35	1.7 ± 0.22	1.80 ± 0.58	2.12
-14.5	39	1.9 ± 0.24	3.38 ± 0.86	3.61
-13.5	56	2.8 ± 0.29	5.80 ± 1.33	5.77
-12.5	84	4.0 ± 0.32	9.41 ± 2.14	9.31

^aFrom data in Secker & Harris (1996).

^bFrom data in Ferguson & Sandage (1991).

To view this figure please download the paper version at <http://www.astro.caltech.edu/~cc/gpec3.ps>

FIG. 1.— Montage images of the Perseus galaxies used in this study. The number at the upper left of each image is M_B , while the lower number is the $(B - R)_0$ color, and the number to the far right is the catalog number from Table 1. The solid black bar on each figure is 3'' in length. Please see <http://www.astro.caltech.edu/~cc/gpec3.ps> for this figure.

To view this figure please download the paper
version at <http://www.astro.caltech.edu/~cc/gpec3.ps>

FIG. 1.— continued.

To view this figure please download the paper
version at <http://www.astro.caltech.edu/~cc/gpec3.ps>

FIG. 1.— continued.

To view this figure please download the paper
version at <http://www.astro.caltech.edu/~cc/gpec3.ps>

FIG. 1.— continued.

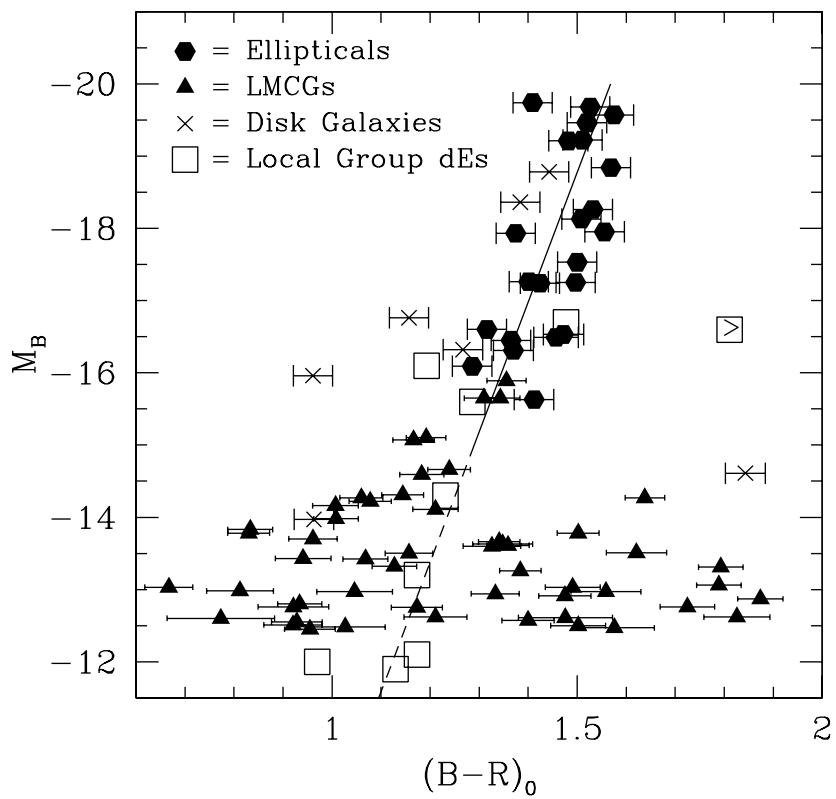


FIG. 2.— The color magnitude diagram for galaxies in the Perseus cluster. Included here are objects with $M_B < -12.5$. All the LMCGs in Figure 1 are plotted on this diagram. The solid line is the fit between color and magnitude for the brighter objects with $M_B < -16$ and the dashed line is the extension of this fit to fainter magnitudes. Also plotted as open boxes are $(B - R)_0$ colors of Local Group dwarf ellipticals derived from their metallicities using data from van den Bergh (2000). The LG dwarf elliptical at $(B - R)_0 \sim 1.8$ and $M_B \sim -16.5$ is an upper limit.

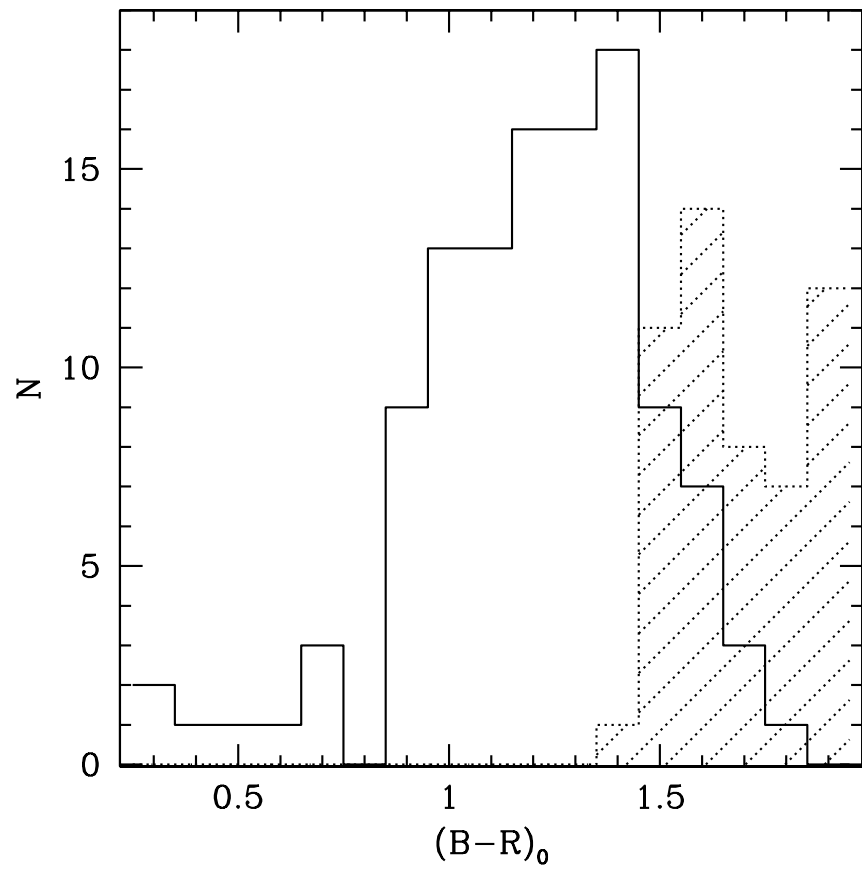


FIG. 3.— Color distribution for all LMCGs in the Perseus cluster center as identified in Paper II, down to $M_B = -11$. The blue (solid) and red (shaded) LMCGs are plotted separately.

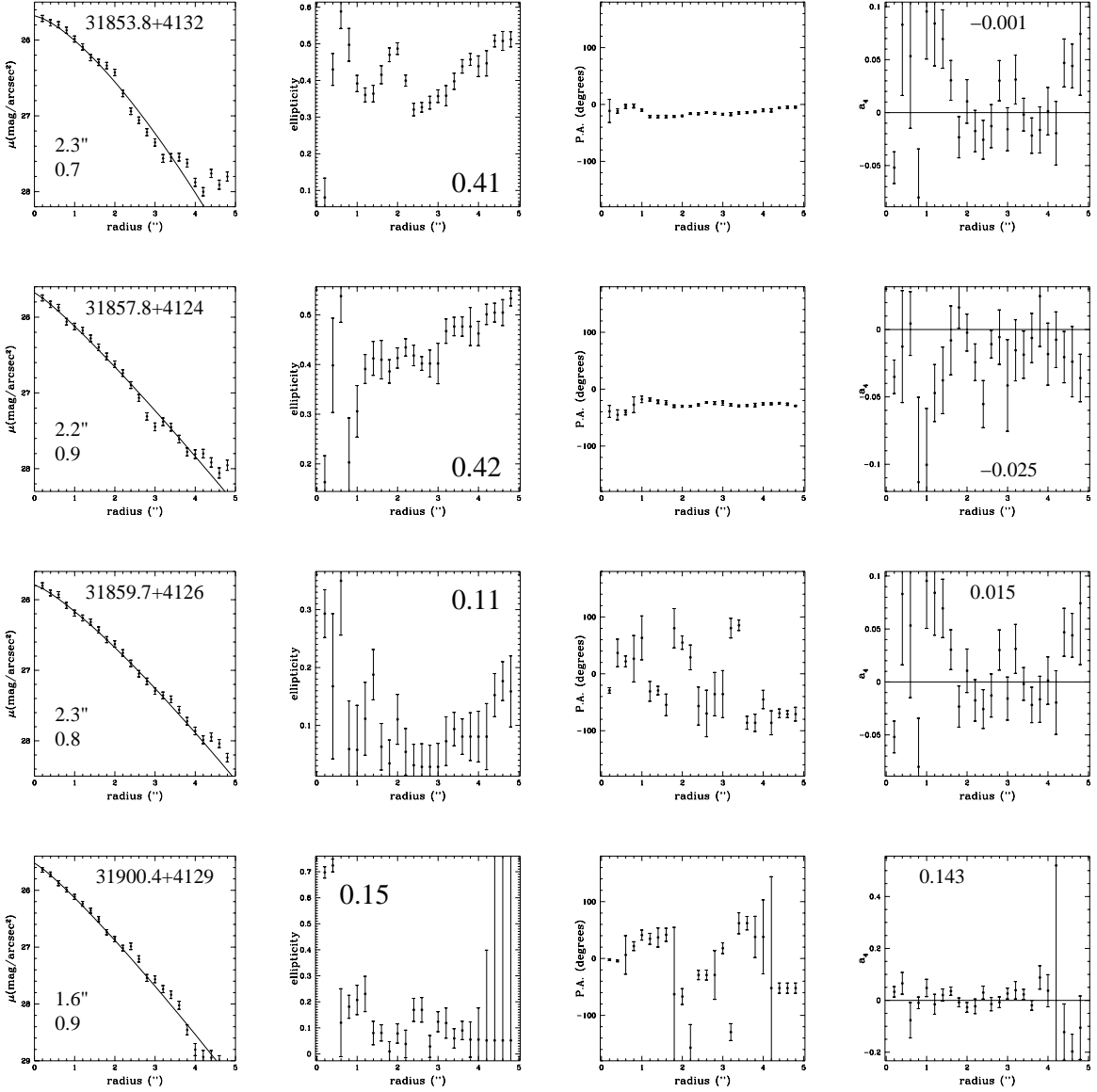


FIG. 4.— Surface brightness profiles, ellipticity profiles, position angles profiles and the a_4 Fourier component profiles for Perseus LMCs with $M_B < -13.5$. The first panel displays the name, Sérsic profile parameters, r_0 and n , for each galaxy. The number in the second and fourth column is the average ellipticities to $5''$ and a_4 value across all radii.

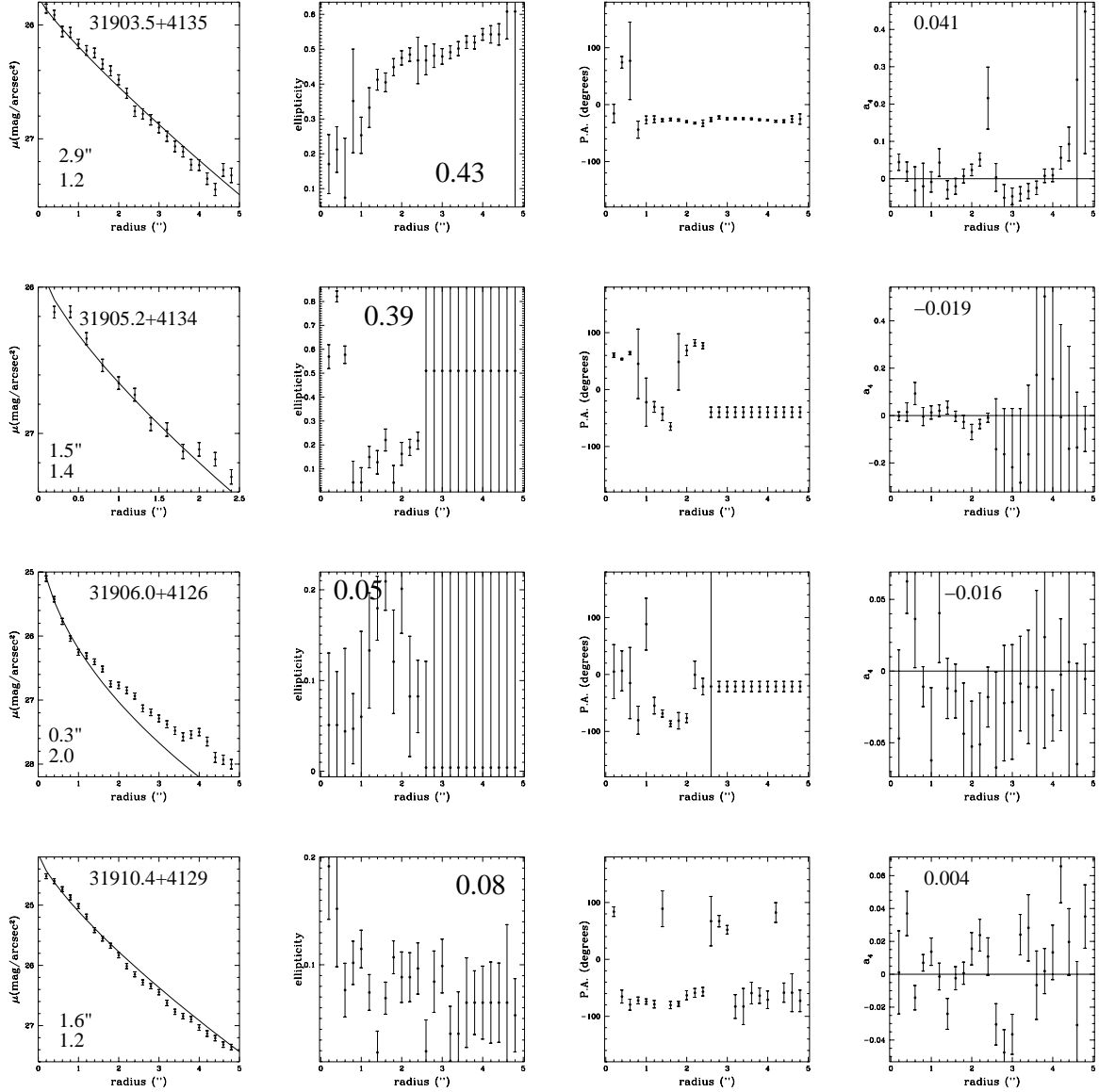


FIG. 4.— continued.

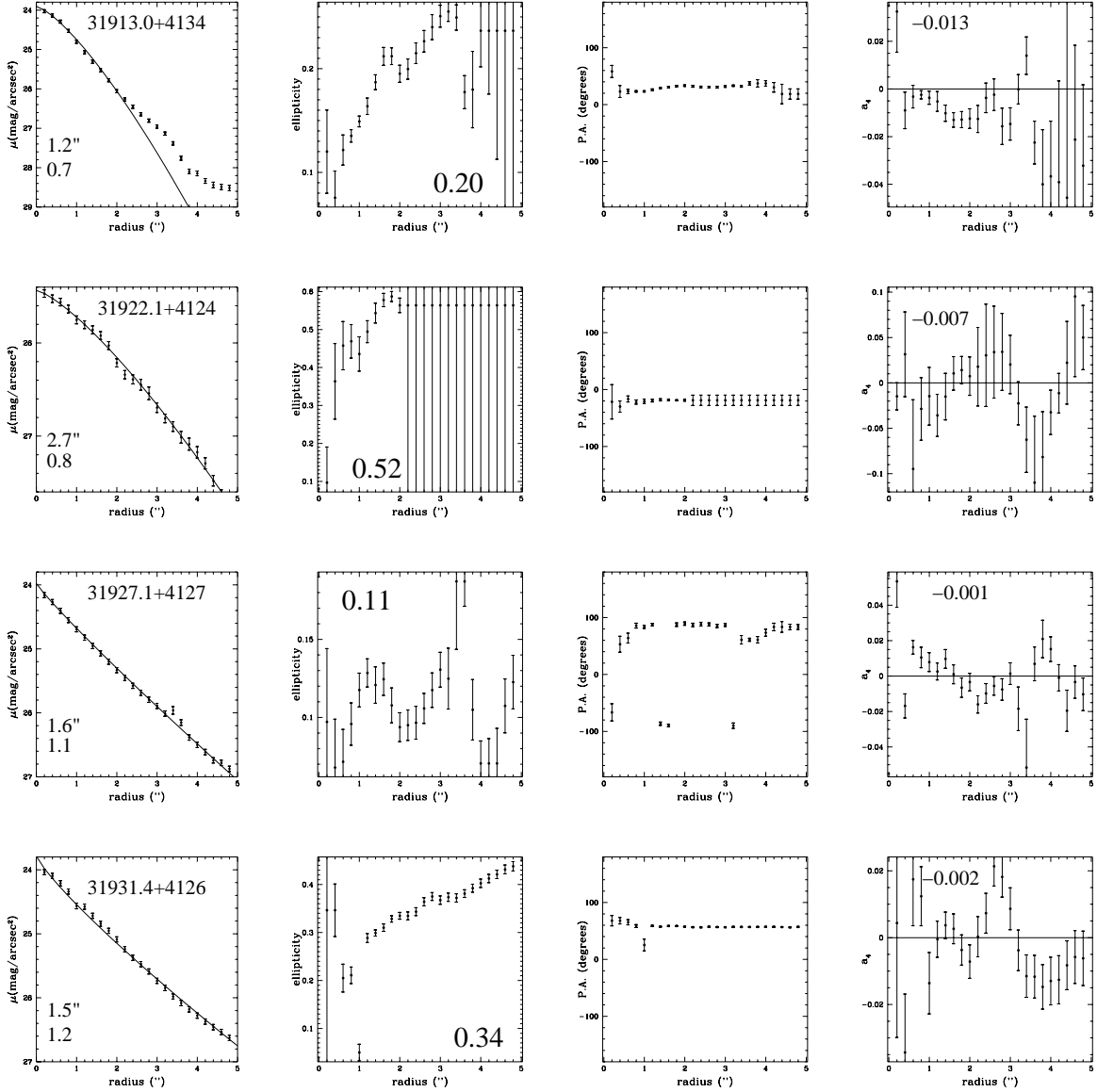


FIG. 4.— continued.

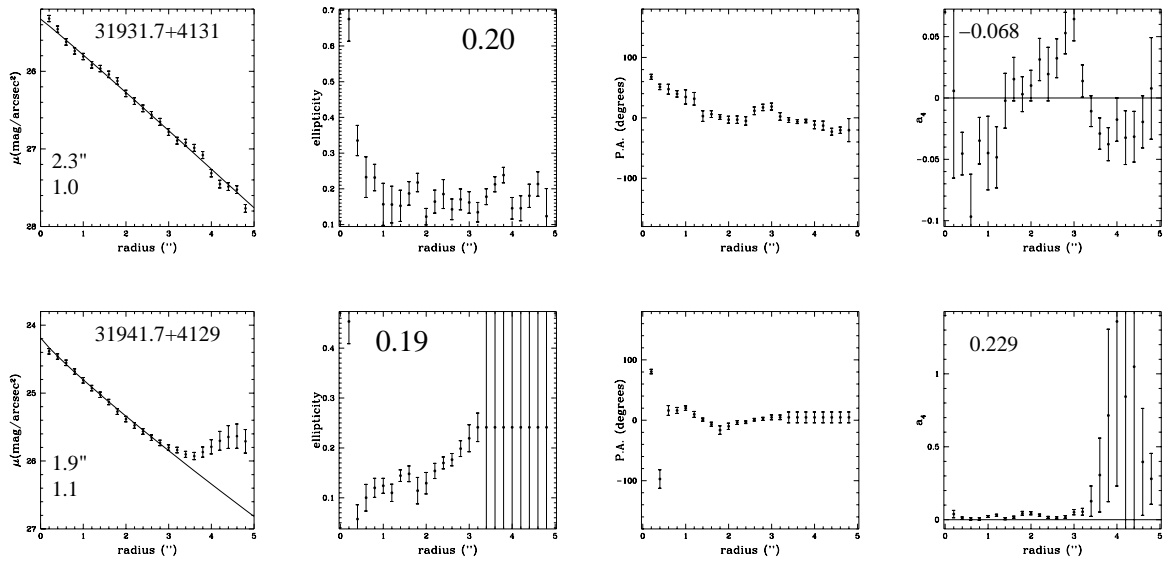


FIG. 4.— continued.

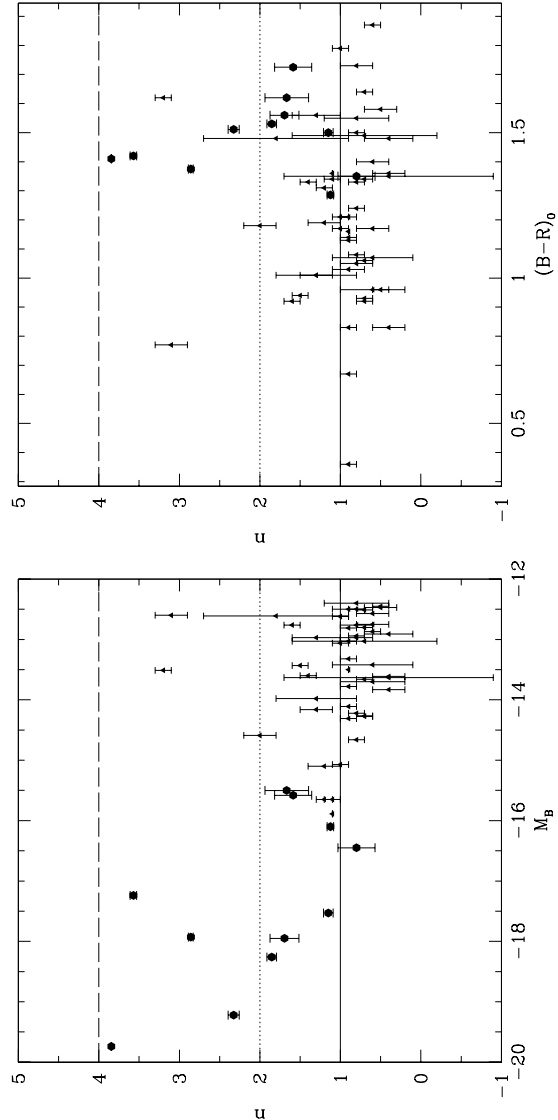


FIG. 5.— Sérsic index n as a function of absolute magnitude M_B (left panel) and $(B - R)_0$ color (right panel) for Perseus LMCs. Symbols are the same as in Figure 2 with the triangle representing the LMCs and the sexagons the giant ellipticals. The long dashed line shows the de Vaucouleur $n = 4$ limit while the $n = 2$ limit for dwarf ellipticals is shown as the dashed line and the exponential profile of $n = 1$ is shown as the solid line.

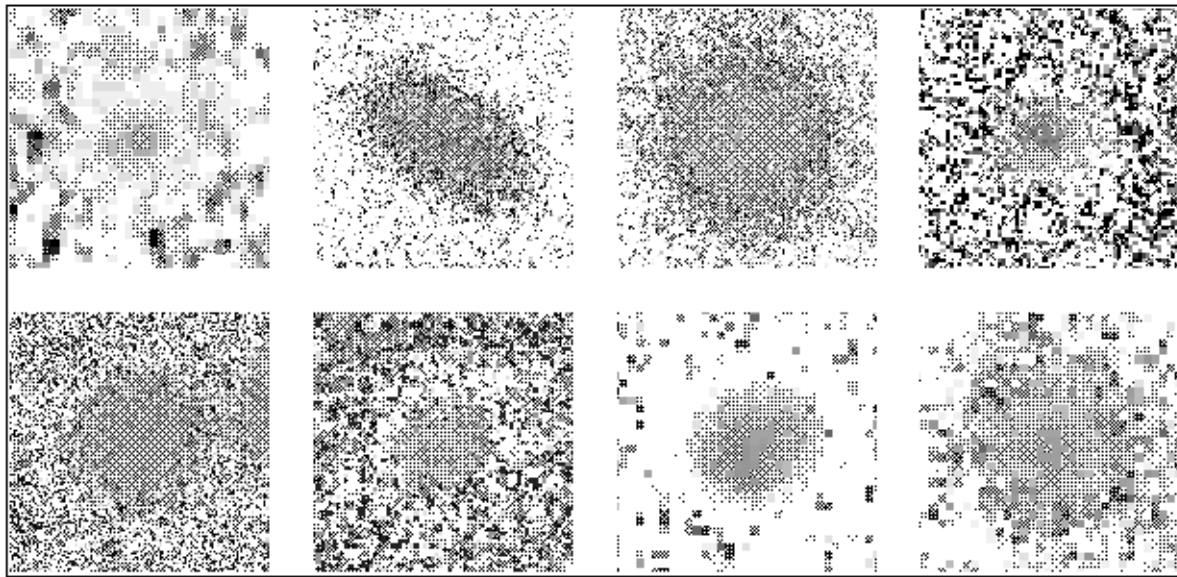


FIG. 6.— $(B - R)$ color maps for bright Perseus LMCGs. Several of these objects are nucleated, but none show large color gradients or distinct core colors. Please see <http://www.astro.caltech.edu/~cc/gpec3.ps> for a much better version of this figure.

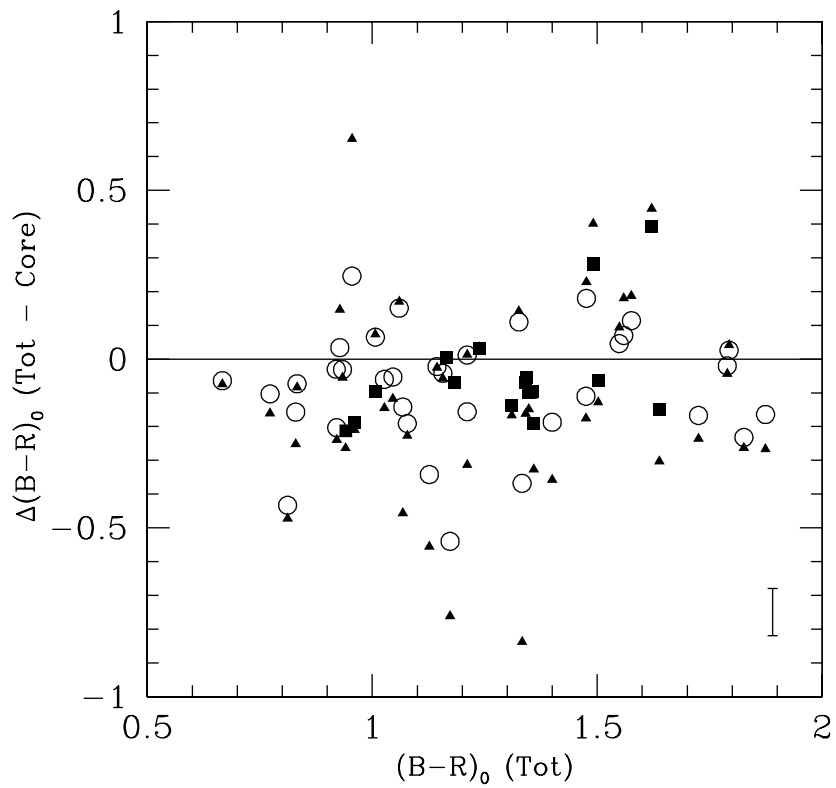


FIG. 7.— The difference in $(B - R)_0$ color between LMCGs and their cores. The solid boxes are nucleated LMCGs while the open circles are the non-nucleated dEs. The solid triangles represent the difference in $(B - R)_0$ between the outer region of each LMCG and their core region.

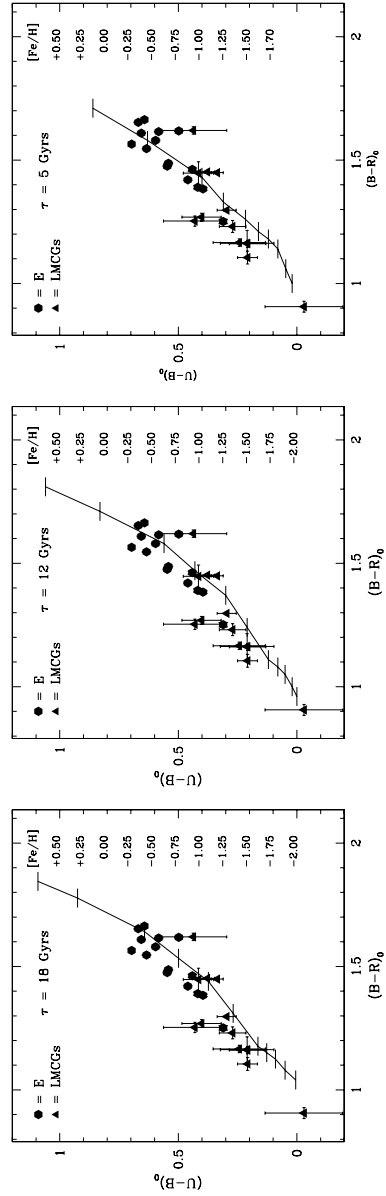


FIG. 8.— UBR color-color diagram for Perseus cluster galaxies plotted with Worthey isochrones at three different ages: 18 Gyr, 12 Gyr and 5 Gyr at metallicities from $[\text{Fe}/\text{H}] = 0.5$ to -2. The horizontal lines along each isochrone tick off the metallicities listed on the right hand side.

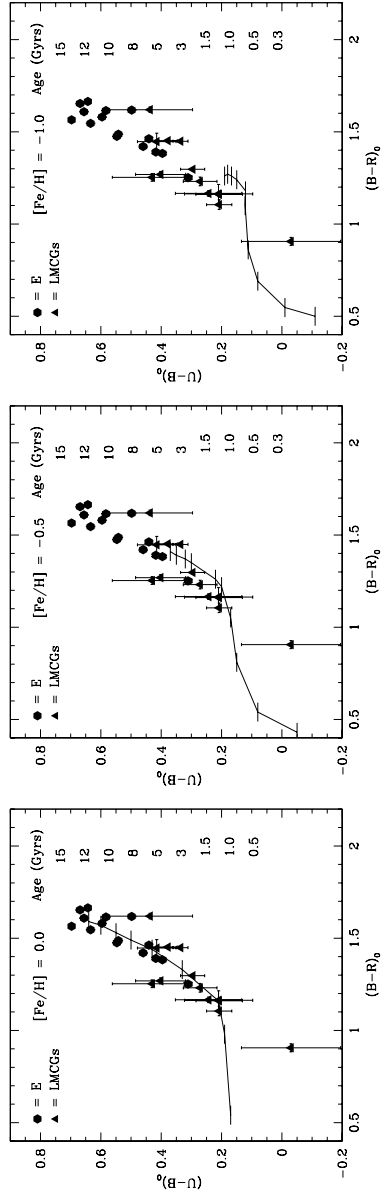


FIG. 9.— Three stellar synthesis modeled age tracks on the UBR diagram at constant metallicities of solar, $[Fe/H] = -0.5$ and $[Fe/H] = -1$. The age range is 0.3 Gyrs to 15 Gyrs for the $[Fe/H] = -0.5$ and -1 models and 0.5 Gyrs to 15 Gyrs for the solar metallicity models.

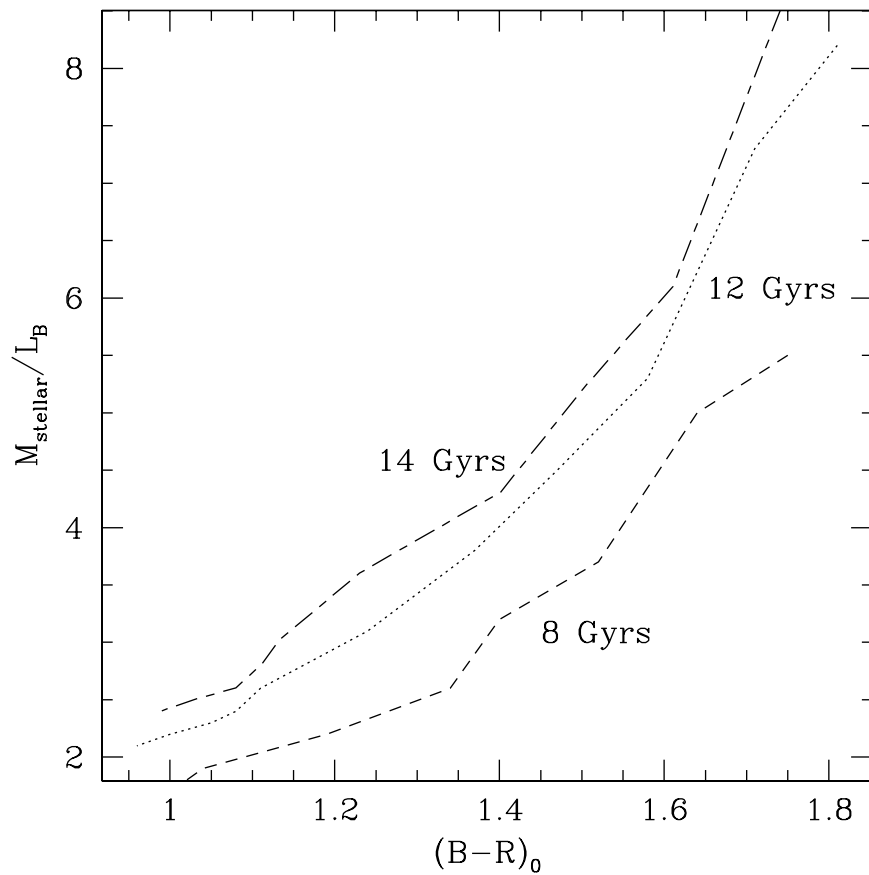


FIG. 10.— The relationship between $(B - R)_0$ color and M_{stellar}/L_B ratios at three different ages using the stellar synthesis models of Worthey (1994) and assuming that color is a measure of metallicity.

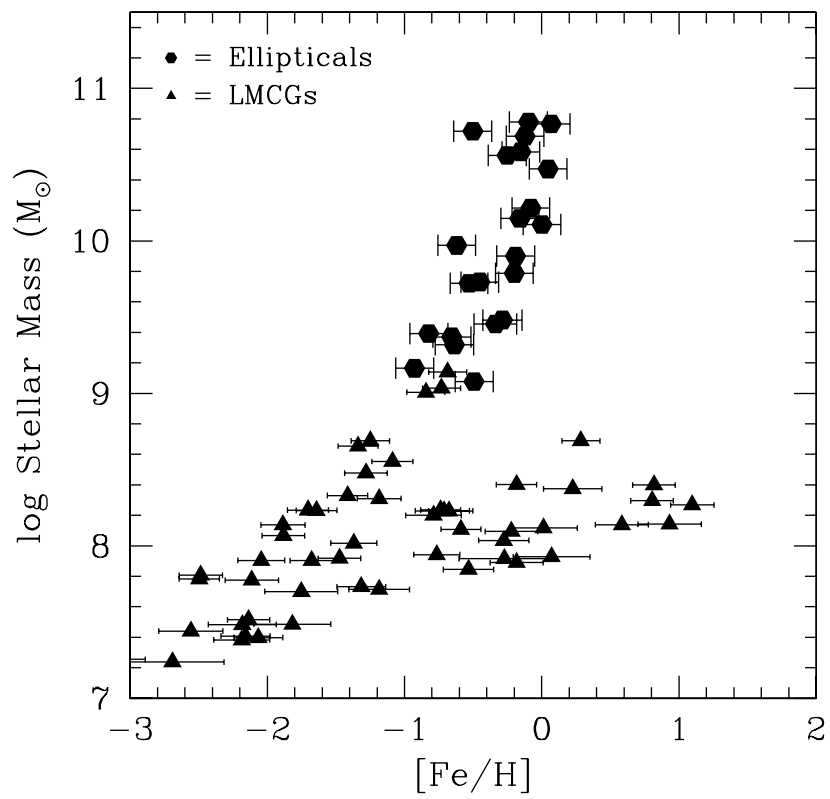


FIG. 11.— The relationship between stellar mass and metallicity for ellipticals and LMCGs in the Perseus cluster. These properties are found by converting $(B - R)_0$ color into metallicity and luminosity into stellar mass by assuming a M_{stellar}/L given by the color (see Text).

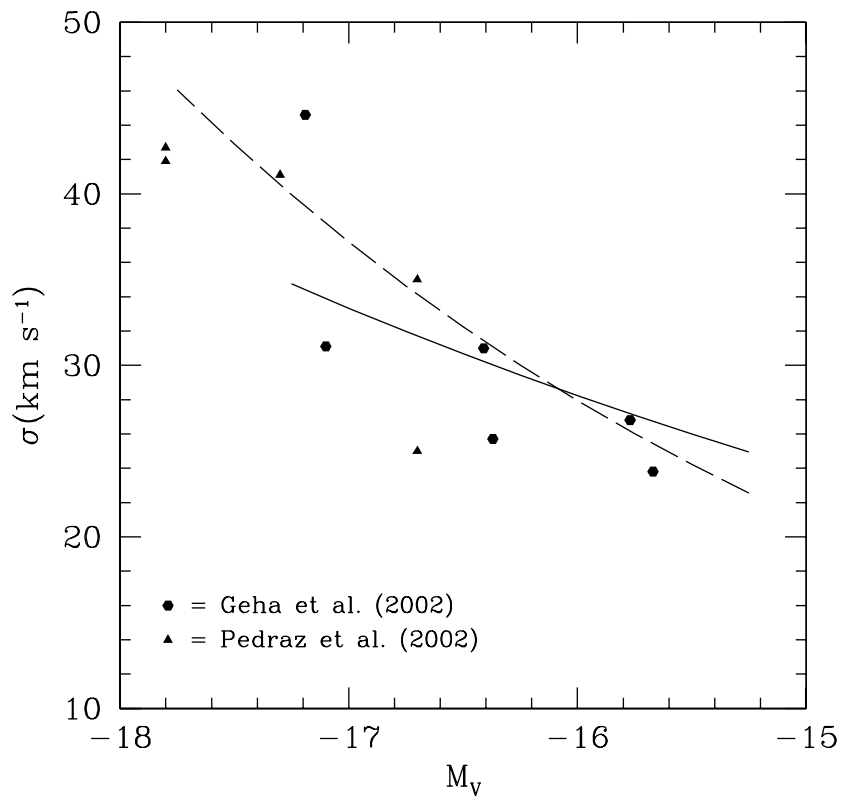


FIG. 12.— The relationship between absolute magnitude M_V and central velocity dispersion σ for Virgo cluster galaxies observed by Geha et al. (2002) and Pedraz et al. (2002). The solid line shows the fit between these two parameters for systems at $M_V > -17$ while the dashed line is the fit for all the galaxies.

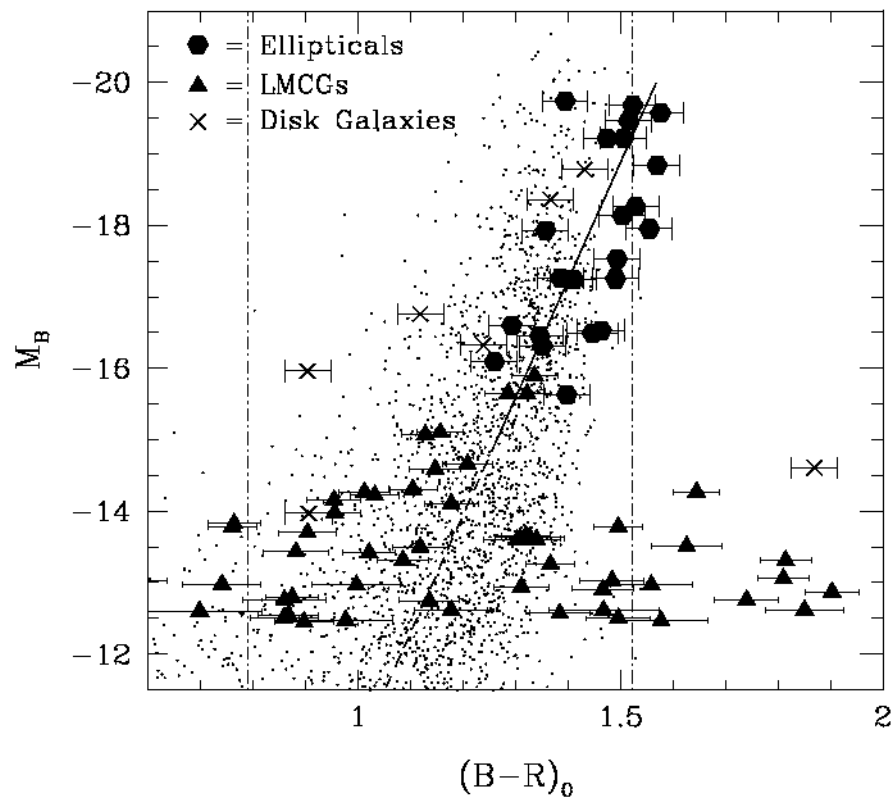


FIG. 13.— The color-magnitude diagram of Perseus galaxies plotted with simulated Λ CDM galaxies from Nagamine et al. (2001). The vertical dot-dashed line shows the limitations of the $(B - R)_0$ metallicity calibration from globular clusters.

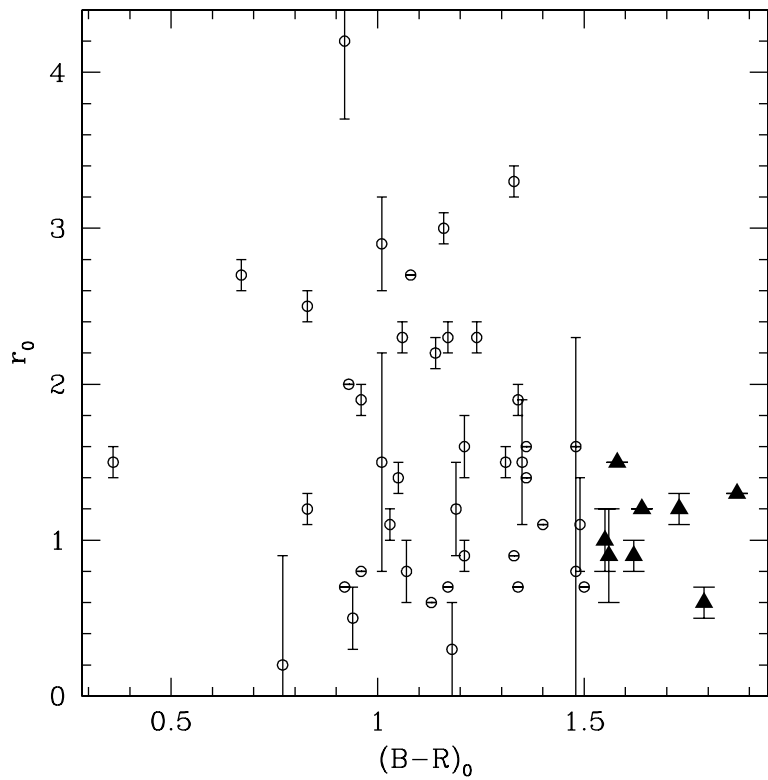


FIG. 14.— Relationship between the Sérsic scale length r_0 and $(B - R)_0$ color for Perseus LMCGs. The open circles are for the blue LMCGs while the triangles are the red LMCGs.

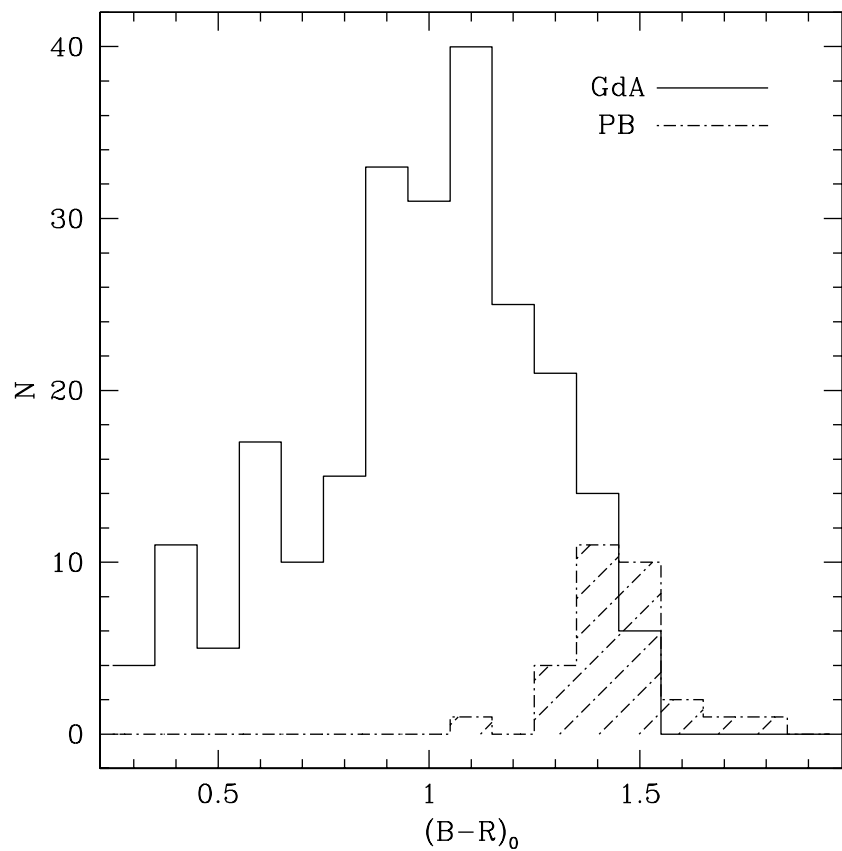


FIG. 15.— Histogram of $(B - R)_0$ colors for spiral galaxy bulges taken from the data in Gadotti & dos Anjos (2001) (GdA) and Peletier & Balcells (1997) (PB).